AD_____

Award Number: DAMD17-01-1-0327

TITLE: Characterization of Breast Masses Using a New Method of Ultrasound Contrast Agent Imaging in 3D Mapping of Vascular Anomalies

PRINCIPAL INVESTIGATOR: Gerald L LeCarpentier, Ph.D.

CONTRACTING ORGANIZATION: The Regents of the University of Michigan
Ann Arbor, MI 48109-1274

REPORT DATE: October 2005

TYPE OF REPORT: Annual

PREPARED FOR: U.S. Army Medical Research and Materiel Command
Fort Detrick, Maryland 21702-5012

REPORT DOCUMENTATION PAGE

Form Approved
OMB No. 0704-0188

1. REPORT DATE *(DD-MM-YYYY)*	2. REPORT TYPE	3. DATES COVERED *(From - To)*
01-10-2005	Annual	24 Sep 04 - 23 Sep 05

4. TITLE AND SUBTITLE
Characterization of Breast Masses Using a New Method of Ultrasound Contrast Agent Imaging in 3D Mapping of Vascular Anomalies

5a. CONTRACT NUMBER

5b. GRANT NUMBER
DAMD17-01-1-0327

5c. PROGRAM ELEMENT NUMBER

6. AUTHOR(S)
Gerald L LeCarpentier, Ph.D.

E-Mail: gllec@umich.edu

5d. PROJECT NUMBER

5e. TASK NUMBER

5f. WORK UNIT NUMBER

7. PERFORMING ORGANIZATION NAME(S) AND ADDRESS(ES)
The Regents of the University of Michigan
Ann Arbor, MI 48109-1274

8. PERFORMING ORGANIZATION REPORT NUMBER

9. SPONSORING / MONITORING AGENCY NAME(S) AND ADDRESS(ES)
U.S. Army Medical Research and Materiel Command
Fort Detrick, Maryland 21702-5012

10. SPONSOR/MONITOR'S ACRONYM(S)

11. SPONSOR/MONITOR'S REPORT NUMBER(S)

12. DISTRIBUTION / AVAILABILITY STATEMENT
Approved for Public Release; Distribution Unlimited

13. SUPPLEMENTARY NOTES

14. ABSTRACT
Doppler ultrasound and other imaging modalities have been used to assess characteristics of vasculature associated with malignant breast masses. 3D contrast refill imaging should help visualize slow-flow in small neo-vasculature associated with these masses. The dual-transducer method proposed should provide vascular mapping while minimizing acquisition time, the major limitation of techniques such as interval-imaging (I-I) and real-time (RT) imaging. Previous phantom tube-flow studies and fixed porcine kidney studies were further analyzed and formalized in two separate papers submitted to Ultrasound in Medicine and Biology. While results were promising, follow-up verification of the latter displayed some unexplainable anomalies. It has become clear that comparisons of mean transit time alone are insufficient. It is also apparent that input contrast signal levels vary in time in less than ideal ways (i.e. as opposed to our earlier assumption of exponential decay). We have begun to evaluate a method for estimating the signal level in 100% blood from characteristics of cumulative histograms of each acquired image. This should allow us a method to both monitor fluctuations of input contrast signal level and calculate a real value for fractional blood volume (and subsequently, combined with mean transit time estimates, an actual measure of perfusion).

15. SUBJECT TERMS
None provided.

16. SECURITY CLASSIFICATION OF:			17. LIMITATION OF ABSTRACT	18. NUMBER OF PAGES	19a. NAME OF RESPONSIBLE PERSON
a. REPORT	b. ABSTRACT	c. THIS PAGE			USAMRMC
U	U	U	UU	70	19b. TELEPHONE NUMBER *(include area code)*

Table of Contents

Introduction

As mentioned in previous annual reports, the overall objective of this project has been to develop a 3D ultrasound contrast imaging system for characterizing suspicious breast masses. The originally proposed method uses a dual-transducer scheme to map mean blood transit time in three dimensions. The method requires a fraction of the time necessary to obtain similar information using other standard contrast imaging techniques, and it should provide information related to normal and anomalous vascular characteristics in and around suspicious masses. In addition, the technique should allow visualization of areas of slow flow and microvasculature, which cannot be detected with conventional Doppler imaging methods. It is hypothesized that these measures will enhance our ability to discriminate benign from malignant lesions as well as serve to increase our understanding of tumor biology in terms of vessel formation.

The originally proposed schedule would have concluded at the end of year three; however, a no-cost extension was added for further refinements and clinical trials. Year four was used primarily to further laboratory experimentation and data analysis to understand the 3D contrast imaging. We have formalized these analyses with 2 paper submissions: (1) "Rapid 3D Imaging of Contrast Flow I: Demonstration of a Dual Beam Technique," and (2) "Rapid 3D Imaging of Contrast Flow II: Application to Perfused Kidney Vasculature." These were both submitted to *Ultrasound in Medicine and Biology* and appear in the appendix. A brief discussion of the papers is presented in the report, but the reader is referred to the appendix for detailed introduction, methods, results, and discussion.

Investigations beyond the submitted work indicated that contrast refill was still not understood well enough to commence with clinical trial. A review of highlights of the problems and issues appear below in the report. An additional no-cost extension allowed for more projected time into year five.

Body

Background:

Given that the following background text provides information regarding the impetus of the proposed work, it is essentially unchanged from our previous reports. Other introductory comments can be found in the two papers in the appendix. As mentioned in the original proposal and other yearly reports, previous studies by other investigators have demonstrated characteristics of vasculature associated with malignant breast masses. These have included thin-walled blood vessels, increased microvessel density, disordered neo-vascularization penetrating the mass, arteriovenous shunting, and a variety of characteristic Doppler

ultrasound and histologic findings [Lee et al. 1996, Peters-Engl et al. 1998]. Some studies strongly suggest that flow velocity demonstrates significant correlation with tumor size [Peters-Engl et al. 1998] and that parameters such as vessel count and flow velocity display significant differences between malignant and benign lesions [Madjar et al. 1994]. A shortcoming of most of these trials has been the limitation of 2D images in assessing overall vascular morphology, density, and velocity distributions.

Given the limitation of 2D studies and the relative sparseness of breast vasculature, our group has investigated the utility of 3D breast imaging for several years. Recently published results [LeCarpentier et al. 1999] indicate that one of our Doppler vascularity measures, Speed Weighted pixel Density (SWD), is statistically different for benign versus malignant lesions and comparable to ultrasound grayscale (GS) evaluation. More recent work in a 38 patient pool suggests that multi-variable indices (which include both SWD and GS features) demonstrate good results in differentiating benign from malignant breast masses well beyond GS evaluation alone [Bhatti et al. 2000]. In a follow-up study (submitted and accepted for publication), the results of the initial 38 patients (18 benign, 20 malignant) were used to form a learning set (A), and multivariable indices were established using Bayesian discriminators. In Group A, 94% specificity was achieved for the SWD-Age-GS index at 100% sensitivity. Applying the same linear function to the second pool (B) resulted in 86% specificity at sensitivity of 100% [LeCarpentier et al. 2002]. The diagnostic performance of SWD in our second patient population strongly suggests the utility of vascular indices in the characterization of breast masses.

In addition to Doppler imaging, a number of investigators have performed extensive evaluation of ultrasound contrast agents in the evaluation of blood flow. Success of low-frame-rate imaging (termed "transient response imaging" or "interval imaging") is related to the "refill" of agent into tissue [Porter and Xie 1995, Porter et al. 1997]. Monitoring refilling has estimated the perfusion in tissue [Wei et al. 1998] and specific pulsing sequences such as "Flash Echo Imaging" (Toshiba Medical Systems) and "Power Pulse Inversion" (ATL/Phillips) have been developed on ultrasound scanners to obtain refill information. Studies at our institution

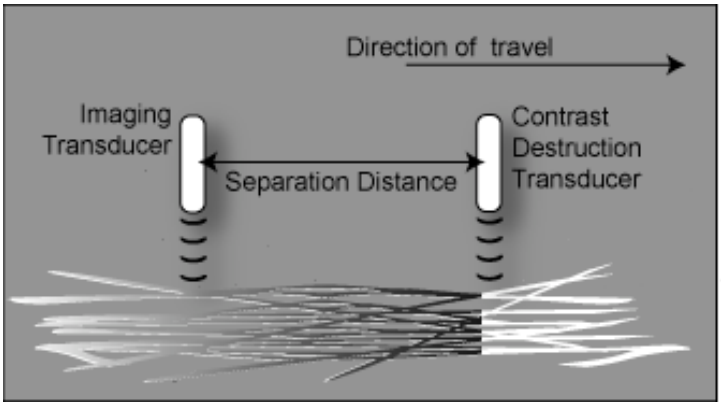

Figure 1. Schematic of dual-transducer method or monitoring capillary refill. The high intensity transducer is used to destroy contrast and create a zero-contrast-enhanced wavefront. The low intensity imaging transducer follows behind at some fixed time (distance). By sequentially scanning the same region using different delays, a refill-time map can be constructed for the volume.

[Fowlkes et al. 1998] have shown that it is possible to destroy contrast agent flow in arteries to produce interruptions with signal separation up to 30 dB. Similar interruptions allow downstream contrast agent to clear and the release of a short bolus by temporarily turning off the field [Rhee et al. 1998]. All of these methods rely on controlled destruction of contrast agents and subsequent reflow into tissue. Complications associated with such measurements in 3D are addressed in this work.

A general scheme of contrast disruption and refill is as follows: An ultrasound beam is used to destroy contrast agent in all vessels in the imaging plane. The larger vessels with significant volume flow and high flow rates quickly refill. The volumes of interest, however, are slower flow in the capillary bed. As the arterioles are filled, the contrast can be visualized, and eventually capillary refill will be seen. Figure 1 depicts the dual-transducer imaging scheme. For the sake of discussion, consider the case of a patient under constant drip infusion of ultrasound contrast agent. At steady state, the imaged blood is 100% contrast enhanced. By translating an ultrasound transducer transmitting a sequence of high-intensity pulses, a wavefront of maximally broken contrast or "zero-contrast-enhanced" tissue is formed. Although the figure shows vessels virtually flowing in the same direction for simplicity, a model will be developed to describe the more "real-world" scenario of isotropically distributed flow into and out of the particular volume of interest. The second transducer, which arrives at the same location at time 2, images the partially refilled volume. This process can be repeated multiple times using different delay settings between contrast destruction and imaging to estimate refill rates for every region in the overall imaged volume.

Specific Tasks:

In the originally proposal document, the approved statement of work included the five major tasks listed below:

Task 1 (months 1-6): Model input function of contrast agent destruction:

(a) Generate mathematical flow model

(b) Measure beam profile

(c) Incorporate various profiles, flow, and scan rates

Task 2 (months 3-12): Assemble and test mechanical imaging scan system:

(a) Design and construct mechanical translation system

(b) Design and test electrical interface

(c) Design and test interface software

Task 3 (months 13-24): Design and perform experimental assessment of imaging system design:

(a) Evaluate performance on strict flow tube models

(b) Evaluate performance on kidney phantom

(c) Evaluate 3 point method of refill curve modelling

Task 4 (months 1-24): Develop and assess visualization and quantification software:

(a) Verify flow model

(b) Develop regional mapping software (*can start as soon as the project begins)

(c) Develop and evaluate parametric histogram visualization scheme

Task 5 (months 13-36): Assess system and 3D imaging software on small patient population:

(a) Recruit patients

(b) Perform scans

(c) Evaluate refill maps and parameterize

(d) Test discriminators

Task 6 (months 30-36): Overall data analysis and write-up

To date, these tasks have been addressed except for the assessment of the imaging system on an actual patient population. Quantification software (Task 4), shown in a previous report, could be modified to use data generated in schemes developed later. Task 3 has been extensively expanded over both year three and the no-cost extension period. As mentioned in the introduction, the analysis and discussion of these aspects appear in the submitted papers in the appendix of this report. Additionally, further analyses of refill characteristics and various inconsistencies were undertaken, and development of methods to normalize measured signal intensities was begun. Initial evaluation of software to re-cast the dual-transducer method to a dual-sweep method for patient studies was performed using hardware developed under a different grant.

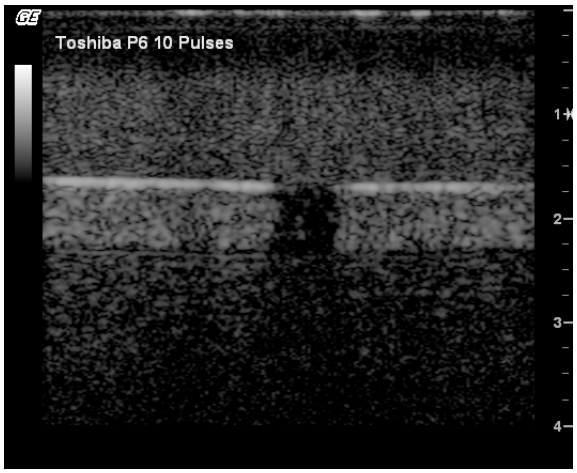

Figure 2. Image of contrast clearance zone thickness. This image, obtained from the imaging transducer at low power shows the 6 mm gap in stationary contrast generated by the clearance transducer after a series of 10 pulses. As such, the effective transducer separation was considered half of the gap (3 mm) less than the physical transducer separation.

Results:

A laboratory set-up and interface software was developed to implement the dual-transducer method described in the introduction and previous reports. The apparatus shown in Figure 4 of the "Demonstration of a Dual Beam Technique" paper in the appendix was used to translate the transducer pair at a constant rate. The distance between the two transducers was varied, and clearance/imaging sequences were performed over a 6.35 mm flow tube and kidney phantom. Contrast clearance zone

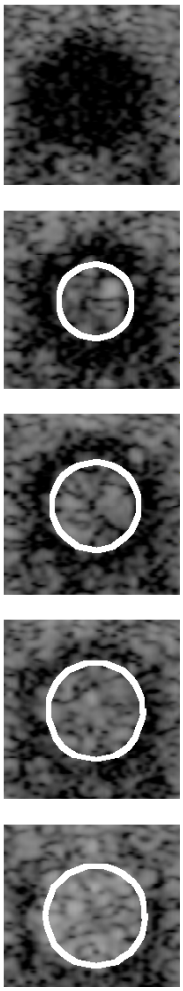

Figure 3. Sample planar images of tube flow. For the 0.040 mL/s flow rate, these images are a sample of those directly obtained in the transducer axial-lateral plane of the flow at a distance d of 16 mm for differing values of Δt. The circles of contrast have observed diameters respectively of 3.36, 4.47, 5.53, and 5.97 mm corresponding to theoretical values (outlined) of 3.67, 4.36, 4.76, and 5.02 mm with increases in Δt.

thickness was imaged by applying multiple pulses to the tube and imaging longitudinally with low power as shown in Figure 2. This provided a "true" transducer separation distance for the analysis. The resulting imaged paraboloid is shown in the appendix. Figure 3 here presents corresponding cross-sectional views, which agree well with expected values. Again, overall results are discussed in the "Demonstration of a Dual Beam Technique" paper in the appendix.

We continued to analyze studies on fixed porcine kidney phantoms as described by Holmes and others [Holmes et al. 1984]. As mentioned previously, the logistics of dehydrating and rehydrating these kidneys were initially problematic. As also continued to be an issue, the stability of contrast agent (Definity) was also problematic given the relatively long (20-30 minute) experimental protocol due to contrast exposure to atmosphere, suspension (stirring) issues, and various pumping parameters. Experimental results were thus interpreted with all of these factors in mind. Specific methods and results are discussed in the "Application to Perfused Kidney Vasculature" paper in the appendix. Of particular interest are example cross-sectional images of the kidney during refill and longitudinal images extracted from the 3D volume as shown in Figures 3 and 7 of the paper, respectively. Reported mean transit times are shown in Figures 5 and 8 of the paper. Comparisons of mean transit times for cross-sectional cases are reproduced here in Figure 4.

The upper bar graph in the figure represents the mean transit times derived from the various methods indicated: the so-called "real-time" imaging, interval-imaging, and the dual-transducer method. Overall, the estimated mean-transit times differ from method to method, but are statistically equivalent for multiple runs within each group where repeated measures were taken. Given our experience with contrast, we had some notion that contrast decay was occurring over time, and all of the measures take some amount of time. In order to make a meaningful comparison, we assumed an exponential decay of the input contrast level and estimated what decay rate would be necessary to show statistical equivalence among the methods. The lower bar graph in the figure represents results of this analysis. Given the

somewhat non-reproducible behavior of the contrast agent with respect to decay over time, the range of values (4.1%/min – 6.2%/min) seemed reasonable. A more detailed discussion can be found in the paper in the appendix.

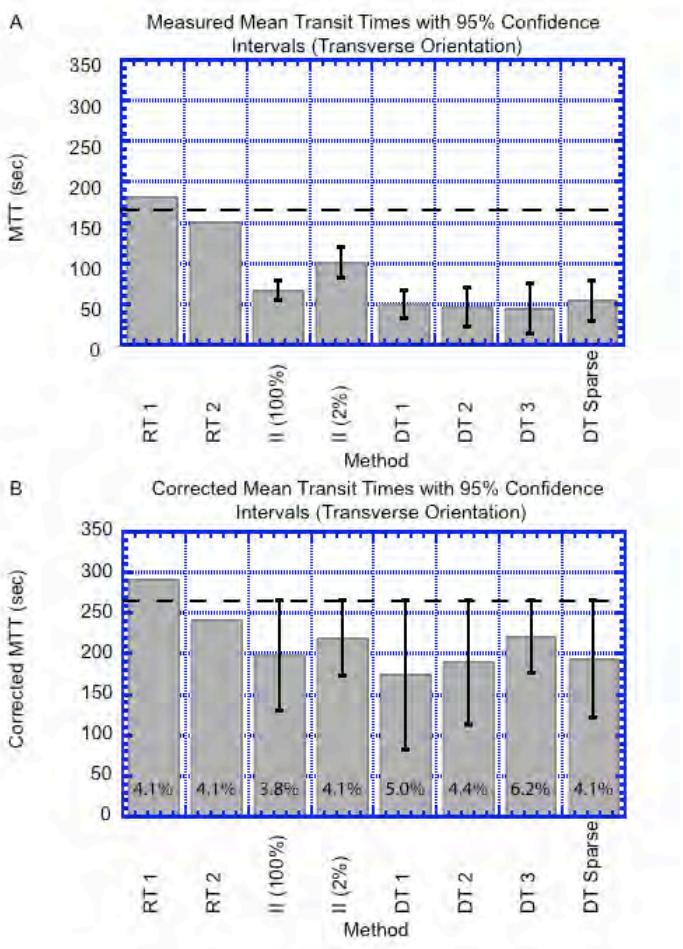

Figure 4. (A) Comparison of data obtained for a given transverse slice, with the ROI (regions of interest) indicated in Figure 8 [of the "Application to Perfused Kidney Vasculature" paper] . Numerals refer to repeated acquisitions using the stated method (e.g. DT 3 - third acquired dual transducer data set). Error bars indicate the 95% confidence interval of the mean transit time value, as fitted to the expression A[1-exp(-1/MTT)] for measured data points. Percentages (for II) refer to the acoustic output (AO) used for readout after set of clearance pulses. Sparse refers to the acquisition where images were obtained at a large (20 mm) slice separation. DT measurements, although differing in absolute terms from corresponding measurements otherwise made, provide a consistent metric of MTT. (B) Factoring in the degradation of contrast agent signal with time, the MTTs can be corrected to values within statistical significance. Because the imaging and flow dynamics are identical for the RT measurements and the II measurement at 2% AO, the MTT should be identical for the measurements. Correcting the RT and II measurements with a contrast degradation factor of 4.1 percent per minute would make the II MTT value statistically equal to the mean of the RT measurements. Applying correction factors (in percent per minute) for the other measurements as indicated would cause the RT MTT mean to be within their 95% confidence interval.

These results, while explainable, are not particularly satisfying. Work on reproducibility was continued after the paper was submitted, and subsequent results will be re-submitted with any revisions. One particular example is that it was noted that the so-called "real-time" refill measurements differed most greatly from the other methods. These were repeated numerous times with varying results. Nonetheless, the "real-time" measures consistently demonstrated an ever-increasing contrast level over time. We have speculated that the "real-time" imaging scheme is not totally non-destructive, and that perhaps contrast agent bubble coalescence is occurring within the kidney phantom model. It may well be that a comparison of other methods to the "real-time" method may be inappropriate. Figure 4 displays a sampling of our results. In these cases, estimation of mean transit time is increasingly uncertain, as the

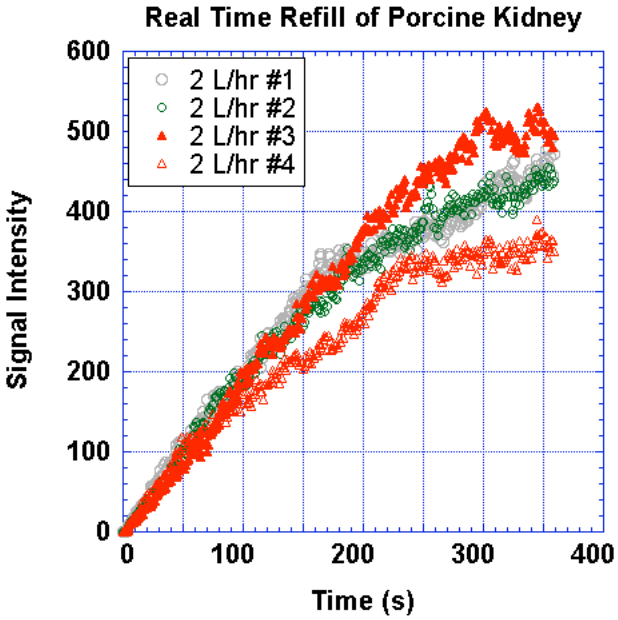

Figure 4. Follow-up refill measurements of porcine kidney observed in "real-time." Asymptotic limit was difficult to perceive in these experimental runs well beyond 300 seconds.

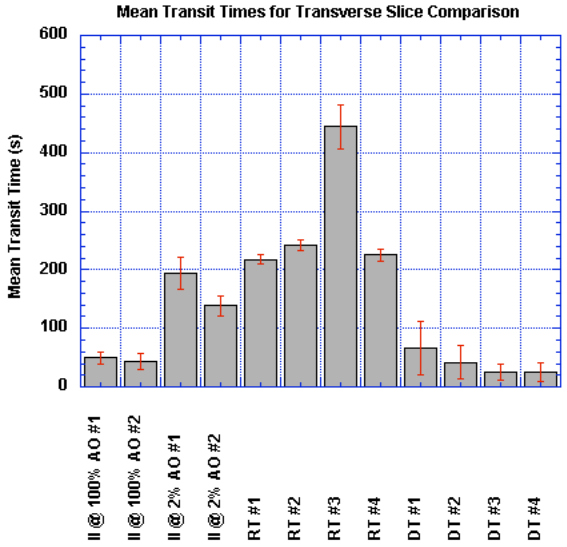

Figure 5. Follow-up mean transit time measurements on porcine kidney. Gross fluctuations were seen particularly with respect to real-time refill characteristics.

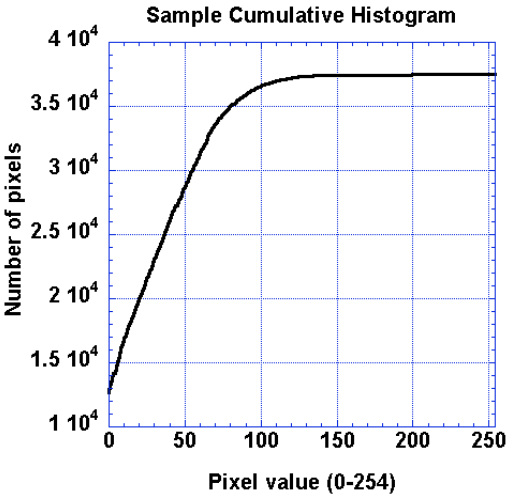

Figure 6. Cumulative histogram of pixel values of a sample interval-imaging case of porcine kidney refill. The best-fit inflection point is used to determine the intensity value of %100 blood.

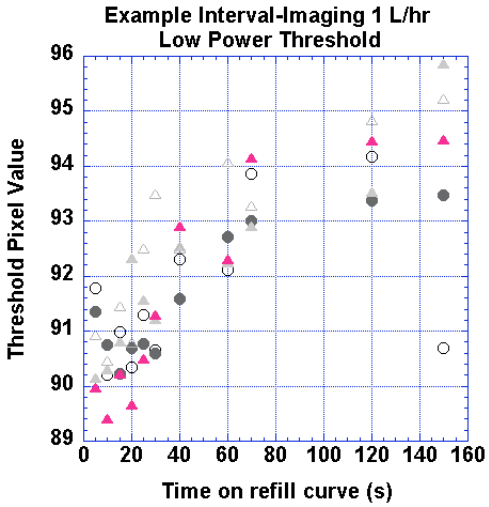

Figure 7. Threshold pixel values as determined from inflection point on cumulative histograms of gray scale pixel values versus refill time. As shown in the graph, threshold values increase only slightly with increasing refill (i.e. increasing contrast agent concentration).

asymptotic limits to the refill are not achieved. Figure 5 shows a follow-up bar graph to that introduced in the paper. In this case, real-time measures are even more divergent than the original report. In addition, the dual-transducer measures are even lower with respect to mean transit time. Note that none of these have been corrected for contrast decay.

From these, we decided that a simple estimate of *possible* contrast decay was inadequate. In fact, if one could estimate the contrast level in 100% "blood," it would be possible not only to

account for input contrast level variations (which may or may not decay exponentially as was assumed in the original paper submission) but also be able to normalize the signal intensities in order to estimate fractional blood volume (FBV). Our mean transit times and the FBV would provide an estimate of perfusion, which is more relevant that MTT alone.

Figure 6 shows an example of a cumulative intensity histogram for a typical porcine kidney image. Considering that 100% "blood" (i.e. in a major vessel) would be display the greatest signal level, the inflection point should indicate that level, as demonstrated by others at our institution. Figure 7 shows how this inflection point varies very slightly with increased contrast level, perhaps owing to partial voluming effects around major vessels as tissue perfuses. At any rate, these initial results appear promising, and we are in the process of determining the best normalization scheme for results to date. Perfusion is in fact the more appropriate marker, and the follow-up research will be aimed at incorporating the perfusion measure into the analysis before clinical trial are undertaken.

Key Research Accomplishments

- Tube flow experiments from previous years were analyzed and formalized in the submitted paper, "Rapid 3D Imaging of Contrast Flow I: Demonstration of a Dual Beam Technique."

- Kidney phantom experiments from previous years were analyzed and formalized in the submitted paper, "Rapid 3D Imaging of Contrast Flow II: Application to Perfused Kidney Vasculature."

- Extensive re-testing of kidney phantom provided insight into possible anomalies displayed in "real-time" refill scenarios, perhaps due to some destruction by low-power ultrasound pulses and possible coalescence of contrast agent bubbles.

- Initial analysis of cumulative histograms of ultrasound scans show promise in determining a value for %100 "blood" for each imaged slice. The impact of this is that we should not only be able account for a varying input contrast signal, but may well be able to actually estimate perfusion.

- Very preliminary results of perfusion measurements display better agreement among the measurement methods. Comparison to "real-time" refill was dropped from the analysis

due to (1) uncertainty regarding our "non-destructive" imaging scheme, and (2) its inherent difference in scheme from the other methods.

Reportable Outcomes

There were two papers submitted to *Ultrasound in Medicine and Biology* and appear in the appendix:

(1) Chen NG, Fowlkes JB, Carson PL, LeCarpentier GL: Rapid 3D Imaging of Contrast Flow I: Demonstration of a Dual Beam Technique.

(2) Chen NG, Fowlkes JB, Carson PL, LeCarpentier GL: Rapid 3D Imaging of Contrast Flow II: Application to Perfused Kidney Vasculature.

Two Abstracts were accepted during the 2004-2005 year:

(1) Chen NG, Fowlkes JB, Carson PL, LeCarpentier GL: Assessment of a 3D Dual-Transducer Ultrasound Contrast Agent Technique for Slow-Flow Vascular Imaging. BMES Annual Meeting, 2005 (accepted).

(2) Chen NG, Fowlkes JB, Carson PL, LeCarpentier GL: A 3D Dual-Transducer Ultrasound Technique for the Assessment of Vascular Flow Using Contrast Agent Imaging. RSNA Annual Meeting, 2005 (accepted).

Conclusions

The dual-transducer technique provides vascular refill information highly correlated to interval and real time imaging, while drastically reducing imaging time required for a 3D volume. The technique may provide measures of refill characteristics in small vessels and slow flow regions where Doppler methods fail. Nonetheless our previous Doppler analysis methods are well suited to contrast agent imaging quantification and breast mass characterization.

There is a time "cost" in obtaining refill data via any clearance/imaging scheme (whether it be interval imaging in 2D or the dual transducer method in 3D), and slow-flow regions may be affected by contrast decay. We have begun to evaluate a method for estimating the signal level

in 100% blood, which should provide us the ability to: (1) monitor fluctuations of input contrast signal level, and (2) calculate a real value for fractional blood volume. The latter, along with our mean transit time estimates will provide a measure of actual perfusion. In our final no-cost extension, we hope to formalize the scheme of normalizing to 100% blood, and begin to apply the method to a small patient pool. We have a single transducer "dual-sweep" hardware apparatus ready to perform this task.

References

Bhatti PT, LeCarpentier GL, Roubidoux MA, Fowlkes JB, Helvie M A, Carson PL: Discrimination of Sonographic Breast Lesions Using Frequency Shift Color Doppler Imaging, Age and Gray Scale Criteria. Journal of Ultrasound in Medicine, 2001, 20:343-350.

Fowlkes JB, Sirkin DW, Ivey JA, Gardner EA, Rhee RT, Rubin JM, Carson PL. Transcutaneous interruption of ultrasound contrast agents for blood flow evaluation. Investigative Radiology 1998 Dec; 33(12):893-901.

Holmes, K. R., Ryan, W., Weinstein, P. and Chen, M. M. A fixation technique for organs to be used as perfused tissue phantoms in bioheat transfer studies. Advances in Bioengineering. R. L. Spiker. New York, Amer. Soc. Mech. Eng. 1984; 9-10.

LeCarpentier GL, Bhatti PT, Fowlkes JB, Roubidoux MA, Moskalik AP, Carson PL. Utility of 3D ultrasound in the discrimination and detection of breast cancer, RSNA EJ, 1999; http://ej.rsna.org/ej3/0103-99.fin/titlepage.html.

LeCarpentier GL, Roubidoux MA, Fowlkes JB, Krücker JF, Paramagul C, Hunt KA, Thorson NJ, Engle KD, Carson PL: Assessment of 3D Doppler Ultrasound Indices in the Classification of Suspicious Breast Lesions Using an Independent Test Population and a 4-Fold Cross Validation Scheme. Radiology 2002 (accepted).

LeCarpentier GL, Chen NG, Fowlkes JB, and Carson PL: Preliminary results of a new method of 3D ultrasound contrast agent mapping of vascular anomalies for characterization of breast masses. Era of Hope, Department of Defense (DOD) Breast Cancer Research Program (BCRP), Orlando FL, September 25-28 2002, P29-6.

LeCarpentier GL, Chen NG, Fowlkes JB, and Carson PL: A new dual-transducer method of 3D ultrasound contrast agent imaging of vascularity. AIUM-hosted 10th Congress of the World Federation for Ultrasound in Medicine and Biology, 2003 (accepted).

Lee WJ, Chu JS, Huang CS, Chang MF, Chang KJ, Chen KM. Breast cancer vascularity: color Doppler sonography and histopathology study. Breast Cancer Research And Treatment 1996; 37(3):291-8.

Madjar H, Prompeler HJ, Sauerbrei W, Wolfarth R, Pfleiderer A. Color Doppler flow criteria of breast lesions. Ultrasound in Medicine and Biology 1994; 20(9):849-58.

Peters-Engl C, Medl M, Mirau M, Wanner C, et al. Color-coded and spectral Doppler flow in breast carcinomas--relationship with the tumor microvasculature. Breast Cancer Research And Treatment 1998 Jan; 47(1):83-9.

Porter TR, Li S, Kricsfeld D, Armbruster RW. Detection of myocardial perfusion in multiple echocardiographic windows with one intravenous injection of microbubbles using transient response second harmonic imaging. Journal of the American College of Cardiology 1997; 29(4):791-9.

Porter T, Xie F. Transient myocardial contrast after initial exposure to diagnostic ultrasound pressures with minute doses of intravenously injected microbubbles. Demonstration and potential mechanisms. Circulation 1995; 92(9):2391-5.

Rhee RT, Fowlkes JB, Rubin JM, Carson PL. Disruption of contrast agents using pulsed ultrasound. J. Ultrasound Med 1998; 16:S97.

Wei K, Jayaweera AR, Firoozan S, Linka A, Skyba DM, Kaul S. Quantification of Myocardial Blood Flow With Ultrasound-Induced Destruction of Microbubbles Administered as a Constant Venous Infusion. Circulation , 1998; 97(5):473-483.

Appendix

Rapid 3D Imaging of Contrast Flow I: Demonstration of a Dual Beam Technique

Chen NG†, Fowlkes JB†‡, Carson PL†‡, LeCarpentier GL‡

Departments of Biomedical Engineering†/Radiology‡, University of Michigan, Ann Arbor, MI, USA

Please send all correspondence to:

Gerald L LeCarpentier, PhD

University of Michigan Dept of Radiology

Basic Radiological Sciences

200 Zina Pitcher Place Rm 3315

Ann Arbor, MI 48109-0553

(734) 647-9326 (Telephone)

(734) 764-8541 (FAX)

gllec@umich.edu

Rapid 3D Imaging of Contrast Flow I: Demonstration of a Dual Beam Technique

Abstract

Perfusion imaging in a 3D volume using ultrasound contrast agent may improve vascular characterization compared to 2D imaging. Conventional 3D acquisition at even modest refill times requires excessive scan time. A dual transducer technique using conventional systems has been introduced that allows 3D imaging of contrast dynamics with drastically reduced scan times (LeCarpentier et al. 2003). Two transducers are translated across a volume where the leading transducer effects contrast clearance and the following transducer images at desired contrast refill times. With 2D arrays that allow simultaneous clearance and imaging pulses, scan times could be further reduced and the need for two transducers eliminated. The dual transducer technique was demonstrated on a tube phantom, with observed contrast profiles closely matching those expected. This technique is introduced for rapid acquisition of 3D contrast refill images and is readily adaptable to systems that allow for the combination of separate clearance and imaging pulses.

Keywords: contrast refill, perfusion, blood flow, imaging, vasculature, angiogenesis

Introduction

Earlier studies have suggested that malignant masses have deviant vasculature including thin-walled blood vessels, increased microvessel density, disordered neovascularization penetrating the mass, arteriovenous shunting, and other histologic findings (Bell et al. 1995; Cosgrove et al. 1990, 1993; Delorme et al. 1995; Kedar et al. 1995, 1996; Lee et al. 1996; Peters-Engl et al. 1998; Vaupel et al. 1989). Visualization and mapping of the blood flow within and surrounding tumors may provide a means for differentiating between benign and malignant masses. Extensive evaluation of ultrasound contrast agents for the measurement of blood flow has been previously performed (Porter and Xie 1995; Porter et al. 1997; Wei et al. 1998) and is related to the refill of contrast agent into the tissue after contrast clearance. In early studies, refill data were obtained using interval imaging (Kamiyama et al. 1996; Moriyasu et al. 1996; Ohmori et al. 1997; Wei et. al 1998), where a plane is cleared of contrast and allowed to refill for a given time. The process is repeated with different times to gather the images at various refill times. Signal intensities for regions of interest encompassing the image are plotted against their refill times. Fitting these data using a model for refill gives the mean transit time (MTT) of each region of interest. Combining the MTTs for regions throughout the image produces a refill map. Subsequent development of low-powered, essentially non-destructive pulse sequences enables the measurement of refill curves in real-time after clearing the plane, in what is termed real-time refill imaging (Porter et al. 1999; Simpson, Chin, and Burns 1998).

Both of these techniques are capable of gathering refill data for a single imaging plane in a reasonable period. However, a tumor is a three-dimensional mass, and

extending data collection to such volumes is impractical because of tremendous time requirements. Acquisitions that require a modest time *t* for a single plane usually become unfeasible in 3D, since every single imaging plane constituting part of the volume would require *t* to acquire. The volume would also need to be perfused with contrast agent during this entire period.

A technique is described which makes three-dimensional data collection more practical. The technique is demonstrated by sweeping a transducer pair, composed of a clearance transducer and a low-power imaging transducer as a unit at velocity *v* over a contrast perfused tissue volume. The clearance transducer causes contrast to be cleared in the swept volume. Since contrast is continually perfusing, the emptied volume immediately begins to refill with contrast. The imaging transducer reaches the location previously occupied by the clearance transducer in time Δt for all positions. As Δt has elapsed regardless of the position along the volume, the imaging transducer images the state of contrast refill at all positions for time Δt after each sweep. Longer Δt values can be obtained by pausing the sweep immediately before the imaging transducer begins entering the volume of interest. A schematic of the method used to demonstrate the technique is shown in Figure 1. Here, two transducers are used but the procedure could be applied for any approach in which separate clearance and imaging sequences can be combined with the logical extension to 3D imaging systems.

A series of sweeps with varying Δt allows collection of refill images for the volume. The dual-transducer technique requires only slightly more time than single slice interval imaging acquisition, thereby making the visualization and mapping of three-dimensional volumes practical in comparison to single-slice acquisition techniques (see

Table 1 and the Appendix). Slice separation is determined by both acoustic frame rate and translation velocity. Under the normal operating limits of the translation system and scanner, the number of acquired image planes over the volume of interest does not affect the overall acquisition time.

In order to test the effectiveness of the dual-transducer technique for high-speed contrast imaging, flow through a tube phantom was imaged. A cylindrical tube was embedded within tissue mimicking foam, and contrast agent was pumped through at known rates. Since the flow profile through the cylinder is theoretically known, one can compare measured three-dimensional profiles with those expected from theory.

Theoretical Considerations

Laminar, viscous fluid flow through a straight, circular cylinder has a well-known parabolic velocity profile given by

$$u(r) = V_c\left[1 - \left(\frac{r}{R}\right)^2\right] \tag{1}$$

where *u(r)* is the flow velocity at radius *r* from the center, V_c is the center velocity, and *R* the tube radius. This velocity profile is independent of time.

Consider the case presented in Figure 2. If at a given starting position along the cylinder one selects volume elements at uniform position *p=0* at time *t=0* for all *r*, then the position of the elements composing the front *p(r,t)* is simply *tu(r)*. The front continually stretches with increasing *t*. Substitution provides

$$p(r,t) = tu(r) = tV_c\left[1 - \left(\frac{r}{R}\right)^2\right] \tag{2}$$

Letting *d* represent the distance along the tube where the imaging transducer samples the contrast agent radii, with *d=0* being the initial uniform position of the front at *t=0*, solving for the radius *r* as a function of *d* gives the following expression for *r(d,t)*

$$r(d,t) = R\sqrt{1-\frac{d}{tV_c}}. \quad (3)$$

Since the imaging transducer samples contrast radii along the tube as functions of *d* and *t*, the model allows the testing of the dual-transducer technique in imaging three-dimensional flows via a comparison of observed and predicted radii. The actual profile predicted under these imaging conditions can be considered a “time-dilated” parabola as given by Equation 3 and shown in Figure 2.

For a given v_T and *s* (known from the dual-transducer configuration) and an observed time-dilated parabola, one could derive the center flow velocity V_c by substituting the expression v_T - *s* for *d* in Equation 3, reducing *r(d,t)* to a function of only *t*

$$r(d,t) = R\sqrt{1-\frac{d}{tV_c}} \rightarrow r(t) = R\sqrt{1-\frac{v_T - s}{tV_c}}. \quad (4)$$

One can fit all the measured radii at their known times *t* to the expression *r(t)*, and estimate the parameter V_c for any given experiment. Comparing the estimated and known V_c values (based on flow rates) provides a measure of the accuracy of the dual transducer technique.

Experimental Methods

All scans were conducted within a water tank lined with sound absorbent rubber and filled with water that had been allowed to come to gas saturation. A schematic of

the overall experimental setup is shown in Figure 3. The phantom was mounted beneath the water on a stand and secured with two rubber bands. A dual transducer assembly is shown in Figure 4 and was constructed using two stepper-motors and controls (Microkinetics Corporation, Kennesaw GA, USA). The motors were controlled from a laptop computer through LabVIEW (National Instruments Corporation, Austin TX, USA) scripts and the DAQCard-700 (National Instruments). The scripts allowed control of both transducer separation and translation along the transducers' elevational direction. The transducer assembly was mounted upon a second stand that placed the transducers above the phantom being scanned.

To build the tube phantom, a block of tissue-mimicking foam (S80 - Crest Foam Industries, Inc. Moonachie, NJ, USA) was saturated with water and frozen in order to temporarily harden the block sufficiently for drilling. A circular hole with a diameter of 6.4 mm was drilled through the block and the foam was subsequently allowed to thaw. Next, a thin-walled (0.79 mm) latex rubber tube with a 6.35 mm inner diameter (Kent Elastomer, Kent, OH, USA) was threaded through the block, with sufficient additional tubing (~20 times diameter) on both ends of the block to dampen transitional flow effects due to connections. The foam block was degassed prior to use by submersion in boiling water and subsequently allowed to cool, after which the phantom was maintained under water at all times.

The tube phantom was connected to form a recirculating flow system using intravenous (IV) tubing. A variable rate IV pump (IVAC 560, IVAC Corporation, San Diego, CA, USA) drove the flow. All flow originated and terminated at a stirred flask containing a contrast suspension (Definity Bristol-Myers Squibb Medical Imaging at a

1:5000 dilution in water). The suspension was continuously circulated through the phantom.

A Toshiba Powervision 8000 scanner (Toshiba Corporation, Otawara-shi, Tochigi-Ken, Japan) with a 3.75 MHz (PVN-375AT) transducer in harmonic mode (power setting of P6 with a frame rate of 10 Hz) was used for contrast clearance. A GE Logiq 9 scanner (General Electric Corporation, Milwaukee, WI, USA) with a 7L transducer in CPI (coded phase inversion) mode was used to image. Since the clearance transducer has a significant contrast disruption zone as indicated in Figure 1, the effective clearance width in the elevational direction of the clearance transducer was measured by stopping the pump, applying a series of frames, and imaging laterally the contrast gap produced using the imaging transducer at low-power (1% acoustic output power setting). Calculations of Δt were based on the distance from the edge of contrast clearance to the center of the imaging transducer. The limit of the clearance width as the number of frames increased without bound was noted as 6 mm and used as the effective width. As such, the effective transducer separation for each scan was considered 3 mm less than the physical transducer separation.

The dual transducer system was used to image the tube phantom at two different flow rates (1.75 and 2.50 mm/sec peak velocity) with effective transducer separations of 42, 57, 72, and 87 mm. Cross-sectional images of the tube phantom were acquired and assembled. Images through the tube center in the lateral-elevational plane were then extracted from the reconstructed 3D imaging volume and scaled appropriately for the transducer translation velocity v_T (6 mm/sec) and frame acquisition rate (19 Hz). Imaged contrast was subsequently compared to expected “time-dilated” parabolae. Observed

and expected profiles were compared visually and quantified by fitting the observed profiles to their corresponding measures of center velocity v_c provided by Equation 4. This lateral-elevational plane was selected for comparison to avoid asymmetric effects of overlying attenuation on the contrast profile. In addition, overlying attenuation due to contrast is eliminated at the profile edge, and a constant point-spread function is maintained throughout the plane.

Results

Representative composite images of time-dilated parabolas assembled from the cross-sectional images with their expected contrast outlines superimposed are shown in Figure 5 for each sweep, with the flow rate and effective transducer separation noted. Since the transducer translation velocity v_T (6 mm/sec throughout) was greater than the maximum flow velocity v_c, the imaging transducer reached and overtook the refilling front for each sweep. At all times, the radius of the observed contrast should be that found by Equation 3. As expected, for the reduced flow rate shown in Figure 5B, the contrast profile does not progress as far as that for an identical Δt (14.5 sec). Examination of the images in Figure 5 reveals a generally good match between the observed profiles and those predicted with the clear exception being the axial center of each profile. The center of the profile does not progress as far as the prediction, and the discrepancy is greater for higher flow rates. Fitting the measured radii to Equation 4 to estimate v_c gives estimated values shown in Figure 6 for all scans acquired. The measured values of v_c are generally somewhat less than their theoretical value.

The slight discrepancy between the expected and observed contrast profiles within the cylindrical tube phantom is probably due to some minimal amount of contrast clearance from repeated low-power ultrasound exposure during the imaging process. Contrast clearance is more pronounced near the center of the tube than at the edges, due to the reduction in relative velocities between the flow and transducer. The reduction in relative velocity causes contrast near the tube center to receive more exposure, and hence preferentially clearing it relative to other contrast as shown in Figure 7. In addition, the reduction in overlying attenuation at the axial center also contributes to increased contrast clearance. In spite of the effects of slight contrast clearance, peak flow velocity was measured on average to within 13.2% of that expected.

Conclusions and Discussion

We have demonstrated the efficacy of a new technique in contrast refill imaging. The dual transducer technique allows the imaging of contrast destruction/refill data in a three-dimensional volume in a drastically reduced time frame, compared to traditional techniques (real-time refill and interval imaging). The tube phantom provided a four-dimensional model that allowed the verification of the dual-transducer technique by comparing expected and observed contrast profiles. Fitting observed profile radii to those predicted by Equation 4 gave center velocity measurements v_c measurements that were somewhat less than those expected except for one case (Δt = 14.5 sec, 0.040 mL/sec flow rate). The v_c measurements probably tended to be low because of slight contrast clearance, which is exhibited in two ways. Looking closely at Figure 5, one

notes first that the observed profiles were truncated at their center. Second, the edge of the contrast profile tended to fall on or within ($r \leq r_{expected}$) the theoretical edge. Radii measurements less than those expected would depress the fitted v_c value.

The exception to the depressed v_c measurements is notable in that the observed contrast profile exceeds ($r > r_{expected}$) the theoretical curve in places, and that the profile is notably brighter than the others. The increase in brightness could be due to higher contrast agent concentration for that scan. Without adjusting for this brightness increase, the observed edge for a given threshold would be farther from the center due to partial volume effects. This increase in the observed radii would then raise the fitted v_c.

We have shown that the technique gives expected results in the laminar tube flow phantom. The dual transducer technique was introduced as a method for high-speed refill imaging. In part II, the application of the technique toward a perfused vascular bed will be examined.

Acknowledgement

This project was sponsored by the US Army under grant DAMD17-01-1-0327 and R01-DK56658 from the US National Institutes of Health (NIH).

References

Bell DS, Bamber JC, Eckersley RJ. Segmentation and analysis of colour Doppler images of tumour vasculature. Ultrasound Med Biol 1995; 21(5): 635-647.

Cosgrove DO, Bamber JC, Davey JB, McKinna JA, Sinnett HD. Color Doppler signals from breast tumors. Work in progress. Radiology 1990; 176(1): 175-180.

Cosgrove DO, Kedar RP, Bamber JC, et al. Breast Diseases - Color Doppler US in Differential-Diagnosis. Radiology 1993; 189(1): 99-104.

Delorme S, Weisser G, Zuna I, et al. Quantitative characterization of color Doppler images: Reproducibility, accuracy and limitations. J Clin Ultrasound 1995; 23(9): 537-550.

Kamiyama N, Moriyasu F, Kono Y, et al. Investigation of the “flash echo” signal associated with a US contrast agent. Radiology Suppl. S 1996; 201: 165.

Kedar RP, Cosgrove DO, Bamber JC, Bell DS. Automated quantification of color Doppler signals: A preliminary study in breast tumors. Radiology 1995; 197(1): 39-43.

Kedar RP, Cosgrove D, McCready VR, Bamber JC, Carter ER. Microbubble contrast agent for color Doppler US: Effect on breast masses. Work in progress. Radiology 1996; 198(3): 679-686.

LeCarpentier GL, Chen NG, Fowlkes JB, Carson PL: A New Dual-Transducer Method of Three-Dimensional Ultrasound Contrast Agent Imaging of Vascularity. (proceedings of the 10th Congress of the World Federation for Ultrasound in Medicine and Biology) Ultrasound Med Biol 2003; 29(5S): S53.

Lee WJ, Chu JS, Huang CS, et al. Breast cancer vascularity: color Doppler sonography and histopathology study. Breast Cancer Res Treat 1996; 37(3): 291-298.

Moriyasu F, Kono Y, Nada T, et al. Flash echo (passive cavitation) imaging of the liver by using US contrast agents and intermittent scanning sequence. Radiology

Suppl. S 1996; 201: 374.

Ohmori K, Cotter B, Kwan OL, Mizushige K, DeMaria A. Relation of contrast echo intensity and flow velocity to the amplification of contrast opacification produced by intermittent ultrasound transmission. Am Heart J 1997; 134: 1066-1074.

Peters-Engl C, Medl M, Mirau M, et al. A Color-coded and spectral Doppler flow in breast carcinomas-relationship with the tumor microvasculature. Breast Cancer Res Treat 1998; 47(1): 83-89.

Porter T, Xie F. Transient myocardial contrast after initial exposure to diagnostic ultrasound pressures with minute doses of intravenously injected microbubbles. Demonstration and potential mechanisms. Circulation 1995; 92(9): 2391-2395.

Porter TR, Li S, Kricsfeld D, Armbruster RW. Detection of myocardial perfusion in multiple echocardiographic windows with one intravenous injection of microbubbles using transient response second harmonic imaging. J Am Coll Cardiol 1997; 29(4): 791-799.

Porter TR, Li S, Jiang L, Grayburn P, Deligonul U. Real time visualization of myocardial perfusion and wall thickening in humans with intravenous ultrasound contrast and accelerated intermittent harmonic imaging. J Am Soc Echocardiogr 1999; 12: 266-271.

Simpson DH, Burns PN. Perfusion imaging with pulse inversion Doppler and microbubble contrast agents: in vivo studies of the myocardium. IEEE Ultrason Symposium 1998; 2: 1783-1786.

Vaupel P, Kallinowski F, Okunieff P. Blood Flow, Oxygen and Nutrient Supply, and Metabolic Microenvironments of Human Tumors: A Review. Cancer Research

1989; 49: 6449-65.

Wei K, Jayaweera AR, Firoozan S, et al. Quantification of Myocardial Blood Flow With Ultrasound-Induced Destruction of Microbubbles Administered as a Constant Venous Infusion. Circulation 1998; 97(5): 473-483.

Appendix

The required scan times for imaging a three-dimensional volume using interval imaging, real-time refill, and the dual-beam technique (demonstrated here with two transducers) are calculated as follows:

_: slice density (slices/unit length)

T: volume thickness (length units)

N_s: number of slices, $N_s = \rho T$

N_t: number of time points

t_{clear}: contrast clearance time needed for one slice

t_{max}: maximum time point acquired on refill curve

v_T: transducer translation speed (distance/unit time), $v_T = N_t t_{trans}$ (see below)

t_{trans}: time to translate one slice thickness, $t_{trans} = 1/(\_ v_T)$, $t_{trans} \rightarrow 0$ for two dimensional arrays where translation is unnecessary to image the volume and imaging rates are controlled by propagation and other processing considerations.

t_M: time to reach time point *M*, $t_M \leq t_{max}$

t_r: time to return transducers to starting position

For real-time imaging with a one-dimensional array, the time required is

$$N_s\left[t_{clear} + t_{\max} + t_{trans}\right] \quad (5)$$

which is the number of slices N_s multiplied by the time required to acquire one slice (time to clear the plane plus the maximum time point in the refill curve), plus the time needed to translate the transducer one slice thickness. The number of time points acquired is limited only by the transducer frame rate and does not affect the acquisition time.

For interval imaging, the time required is

$$N_s\left[\sum_{M=1}^{N_t}\left(t_{clear}+t_M\right)+t_{trans}\right] \tag{6}$$

where $t_M \le t_{max}$ and the sum is the total time required to obtain the image for all time points t_M. The required time can vary significantly depending on the selection of points t_M.

The time required for the scans using two transducers to demonstrate the dual beam technique is given by

$$\sum_{M=1}^{N_t}\left[N_s t_{trans}+t_M+t_r\right]-t_r \tag{7}$$

where the clearance transducer has traversed the volume in $N_s t_{trans}$ and the imaging transducer arrives at the volume boundary after time t_M. As N_s is moved into the summation, one can understand how a dramatic reduction in required scan time generally takes place compared to conventional real-time and interval acquisition. If imaging and clearance could be alternated between the two transducers, there is no need to return the transducers to their starting position after each sweep. Under such circumstances, t_r would be 0.

Note that the time required with the dual transducer technique does not depend on the number of slices acquired for a given v_T. That is, for a given v_T, an increase in

the number of slices N_s would result in a corresponding decreases in the translation time between slices t_{trans}, and overall acquisition time would remain constant. The velocity v_T is generally constrained by the acoustic frame rate (AFR) and desired slice density ρ, i.e. $v_T \leq AFR/\rho$ rather than by the capabilities of the translation system. The minimum t_M that can be acquired is limited by translation velocity v_T and the minimum transducer separation. Clearance time t_{clear} is not present because the clearance transducer clears the volume as it is swept.

For a 2D array imaging a volume completely contained within its field of view, the scan time required is given by equations 5 and 6 for real-time and interval imaging, respectively (with $N = 1$). The term $t_{trans} \rightarrow 0$ and the imaging rate is limited by the volumetric frame rate and beam propagation considerations. The minimum acquirable t_M is based on the time required to electronically sweep through and read the volume.

Slice Separation (mm)	Number of Time Points (Interval and Dual Transducer Imaging)	Interval Imaging	Dual-Transducer Technique	Real-Time Refill
0.5	3	80 min	1 min 53 sec	40 min
1	3	40 min	1 min 53 sec	20 min
2	3	20 min	1 min 53 sec	10 min
1	5	67 min	3 min 20 sec	20 min

Table 1 - Comparison of required total time for interval imaging, real-time refill, and the dual transducer technique. Constant parameters used to compute the times are a transducer translational velocity v_T of 6 mm/sec, a transducer separation of 60 mm, and a volume of interest thickness of 40 mm. Chosen timepoints for interval imaging and the dual-transducer technique are (in sec) 10, 20, 30 for 3 time points, with the additional points 15 and 25 for 5 time points. Real-time refill imaging acquires all time points continuously up to the maximum time point. Transducer translation time is negligible for real-time refill and interval imaging (~6.5 sec) and is covered in the rounded times. For the dual-transducer case, the transducer pair is moved back to the starting position after the acquisition of each timepoint, except for the final one. Time required to clear contrast is negligible (< 2 sec) for both interval imaging and real-time refill acquisition. Note that using the dual-transducer method causes a dramatic reduction in the time required to image a three-dimensional volume. Since the dual-transducer technique's time requirement is independent of the slice thickness, image slices could be acquired as closely together as necessary without requiring additional time, subject only to the imaging transducer frame rate, unlike traditional techniques.

Figure 1 - Dual transducer method schematic. Each transducer is assigned a separate task, with the clearance transducer translated over the tissue ahead of the imaging one. The clearance transducer is operated at sufficient power and pulse repetition frequency (PRF) to clear the volume of interest of contrast agent during each sweep. The imaging transducer is operated in a minimally destructive mode, and it reads the amount of contrast agent that has refilled since contrast clearance. Both transducers are swept through the volume of interest at constant velocity v. Based on the separation distance s, the refill associated with a specific interval Δt can be measured. Due to significant clearance zone thickness, s' is less than s the transducer center-to-center distance. Additional delay can be added by pausing the sweep after clearance and before imaging.

Figure 2 - Dual transducer tube flow dynamics. (A) At a given time t_1, contrast refilling the tube cleared previously by the clearance transducer forms a parabolic profile. The imaging transducer images a slice of the profile in cross-section at position d_1. Within that cross-section, the refilled contrast has a radius r_1. (B and C) The contrast profile remains parabolic as the tube refills. At times t_2 and t_3, the cross-sections are imaged at positions d_2 and d_3 respectively. Even though the contrast profile at any instant in time t is parabolic, the measured radii r are taken of contrast profiles at *different* times. (D) If the transducer translation velocity v_T were much larger than the flow velocity, the contrast profiles at each time would not substantially evolve, and r would solely be a function of the position d and the initial delay time between contrast clearance and profile imaging. However, there is a simple relationship for $r(d,t)$ when the contrast

profiles evolve significantly, given by $r(d,t)=R\sqrt{(1-d/tV_c)}$, where R and V_c are respectively the tube radius and center flow velocity. Assembling the measured radii from an evolving contrast profile produces a predictable “time-dilated” parabola (shown by the dashed line).

Figure 3 - Schematic of dual-transducer apparatus and experimental setup. The dual-transducer apparatus consists of a dual-transducer positioning stage, which consists of translation (M_T) and separation (M_S) motors. Each motor turns a threaded rod, which translates a platform that contains a transducer holder. The platforms translate within the tracked slide. Motors are connected to a powered control module, which contain the electronics driving the motors. The control module is linked to a laptop computer through the DAQCard-700. Using LabVIEW scripts, transducers are translated as required. The transducers are positioned above the phantom being scanned, with the clearance transducer (T_c) positioned at the edge of the volume of interest. The phantom is continuously perfused with dilute (1:5000 concentration) contrast pumped from a stirred flask.

Figure 4 - Photograph of the constructed dual-transducer apparatus. Two stepper motors turn two threaded rods parallel to each other to move the ultrasound transducers, which are held by the transducer holders shown. Transducer holders translate on a guided slide (400L - THK Corporation Japan). The separation motor, mounted upon a stand, adjusts transducer separation. The stand in turn is translated by the larger translation motor, which controls the sweeps over the volume of interest.

Imaging and clearance transducers are mounted as shown. The complete apparatus was placed above a rubber-lined water tank upon a stand, and cables connect the motors to a control box (not shown), which provided drive power and was in turn controlled by a laptop computer using the DAQCard-700 and LabVIEW scripts.

Figure 5 - Reconstructed images along the length of the flow tube showing the contrast agent flow. These are corrected for the time-dilation effect described in the text and Figure 2. The white line shows the theoretical position of the contrast front. The flow passed through a tube of radius 3.175 mm at a rate of 0.040 mL/sec (A) and 0.028 mL/sec (B). Transducer translation velocity v_T was 6 mm/sec. Expected profiles closely match those observed, except at the center of the leading edge. It is believed that the discrepancy is due to slight contrast destruction due to both increased beam exposure and decreased overlying attenuation from overlying contrast (see text).

Figure 6 - Fitted v_c results for cylindrical tube phantom. Dual transducer scans were acquired for the cylindrical tube phantom with two center flow velocities (1.75 and 2.50 mm/sec - corresponding to the flow rates of 0.0028 and 0.0040 mL/sec respectively from Figure 5) using four different refill times. Shown are the measured values of v_c obtained by fitting measured contrast radii to the equation given in Equation 4 for all measurements. Dashed lines denote theoretically known values of v_c. Measured values of v_c are on average -13.2% of those expected.

Figure 7 - Simplified model of time spent in the ultrasound beam for various flow speeds. Flow speeds are represented in “beam-widths” per second for normalization. Flow velocity V is considered parabolic, with a profile given by $V(r) = V_{max}[1-(r/R)^2]$, where r is the tube radius and V_{max} the maximum velocity. With a stationary transducer, the fluid closest to the tube wall is exposed to the beam for the longest period of time, and these exposure durations decrease with increased flow velocity as shown by the three curves representing V_{max} at 1, 4, and 10 bw/sec. The thicker shaded curve represents what happens as the transducer is translated along the axis of the tube at a speed higher than the maximum flow velocity. In this case, where V_{max} was set to 10 bw/sec and the transducer speed was set to 1.5 times V_{max}, the maximum exposure to the beam occurs at the center of the tube. This may help explain the center peak cut-off of the flow profiles shown in Figure 4. That is, the contrast may be exposed to sufficient pulses in the center to break the bubbles at higher flow velocities. This effect is compounded by the fact that there is also less overlying attenuation due to the profile shape

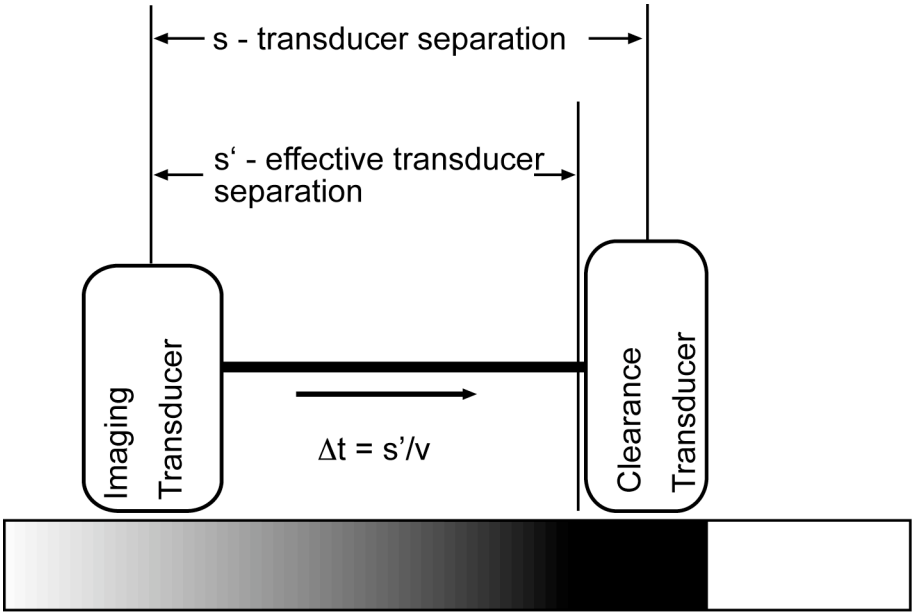
s - transducer separation
s‘ - effective transducer separation
Imaging Transducer
Clearance Transducer
Δt = s’/v

Fig. 1.

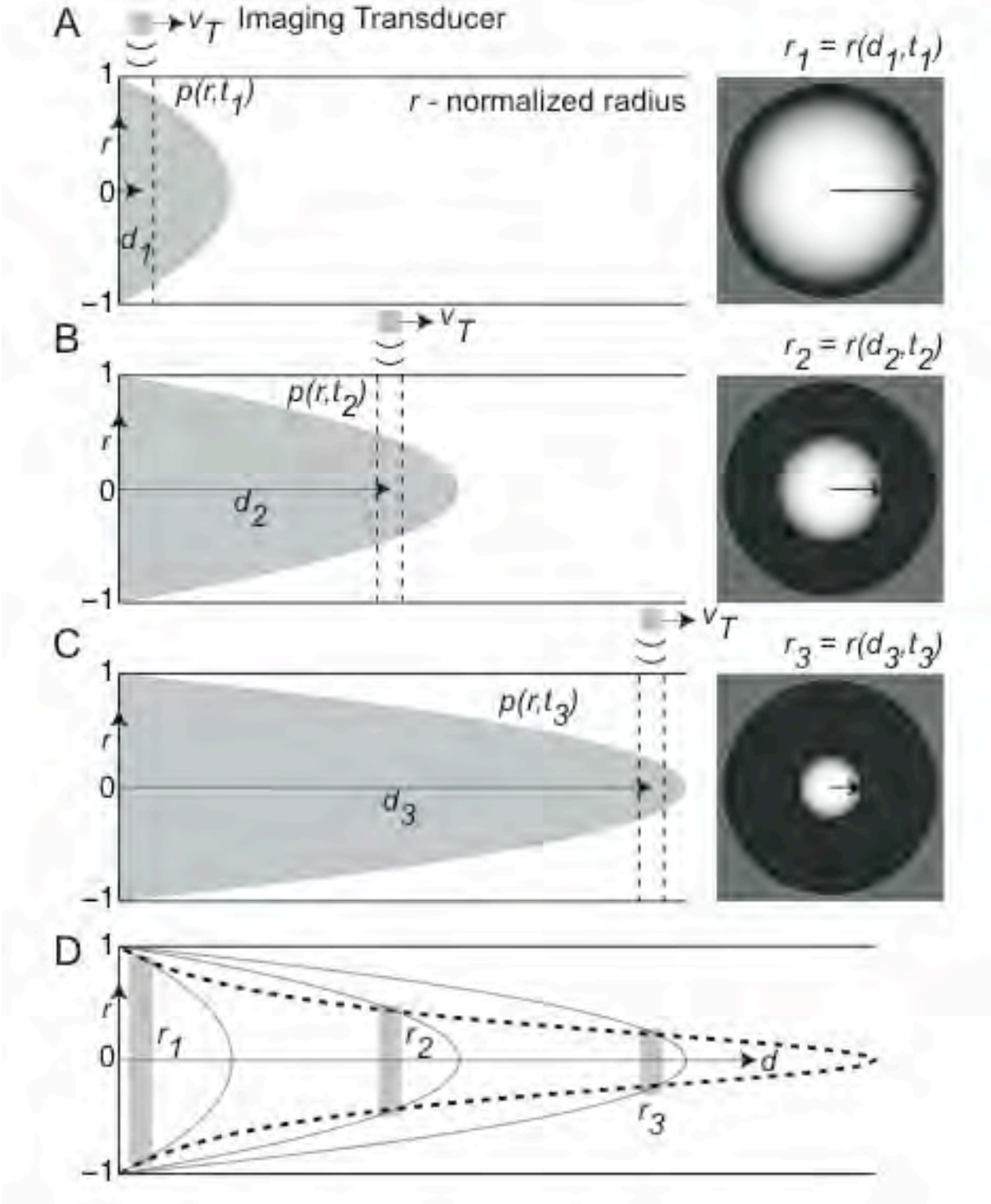
A
v_T Imaging Transducer
$r_1 = r(d_1,t_1)$
$p(r,t_1)$
r - normalized radius
1
r
0
d_1
−1
B
v_T
$r_2 = r(d_2,t_2)$
$p(r,t_2)$
d_2
C
v_T
$r_3 = r(d_3,t_3)$
$p(r,t_3)$
d_3
D
r_1
r_2
r_3
d

Fig. 2.

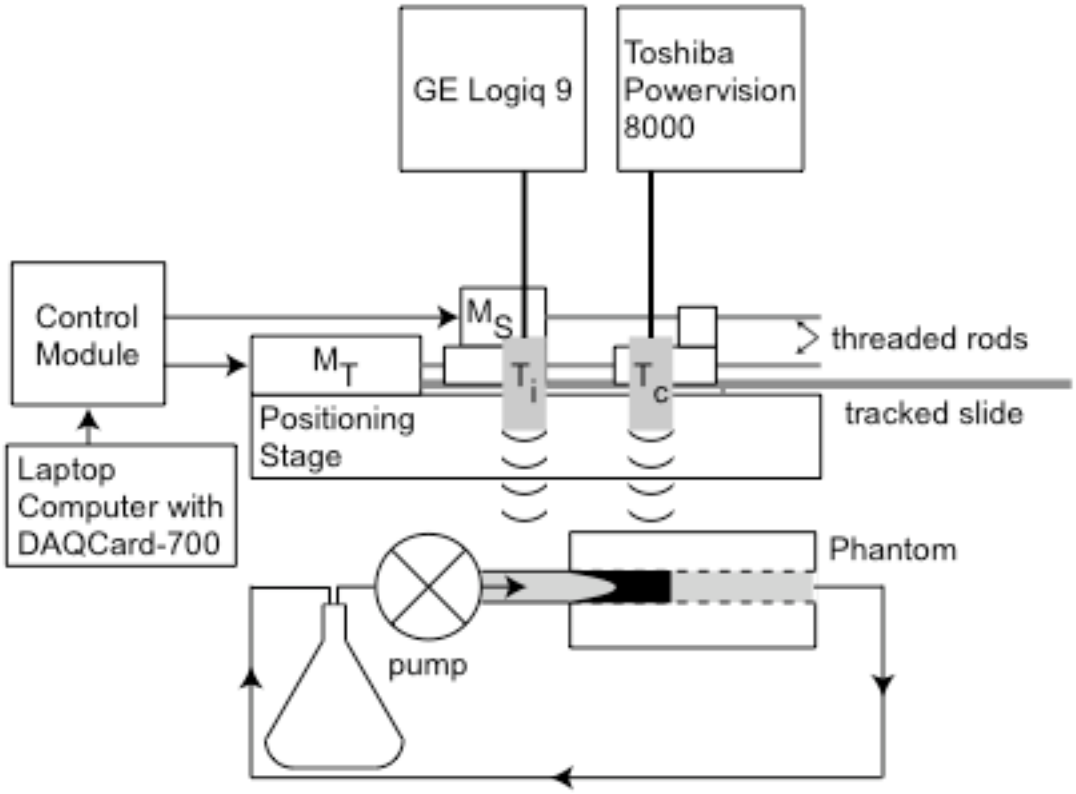
GE Logiq 9
Toshiba
Powervision
8000
Control
Module
M_S
M_T
T_i
T_c
threaded rods
tracked slide
Positioning
Stage
Laptop
Computer with
DAQCard-700
Phantom
pump

Fig. 3.

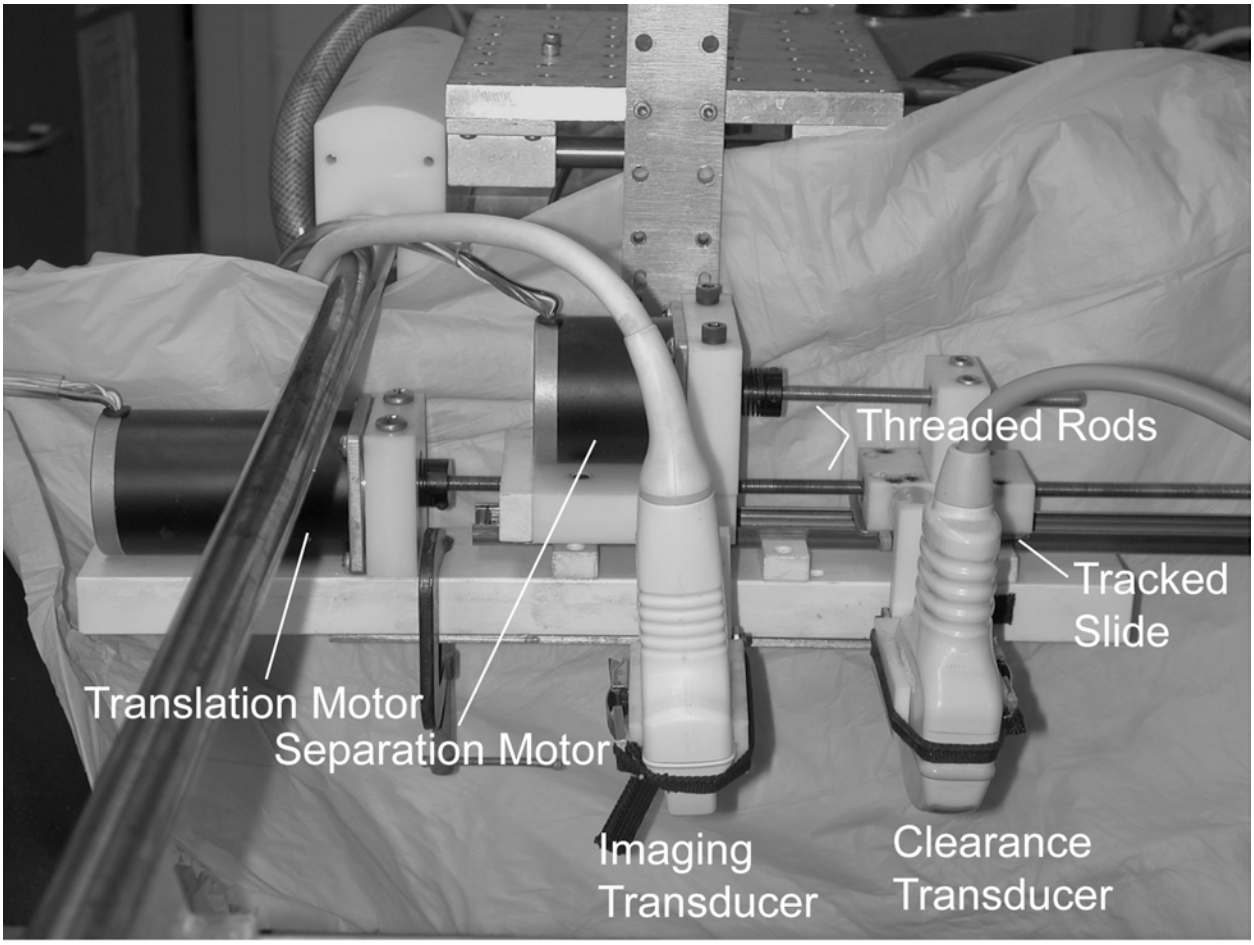
Threaded Rods
Tracked Slide
Translation Motor
Separation Motor
Imaging Transducer
Clearance Transducer

Fig. 4.

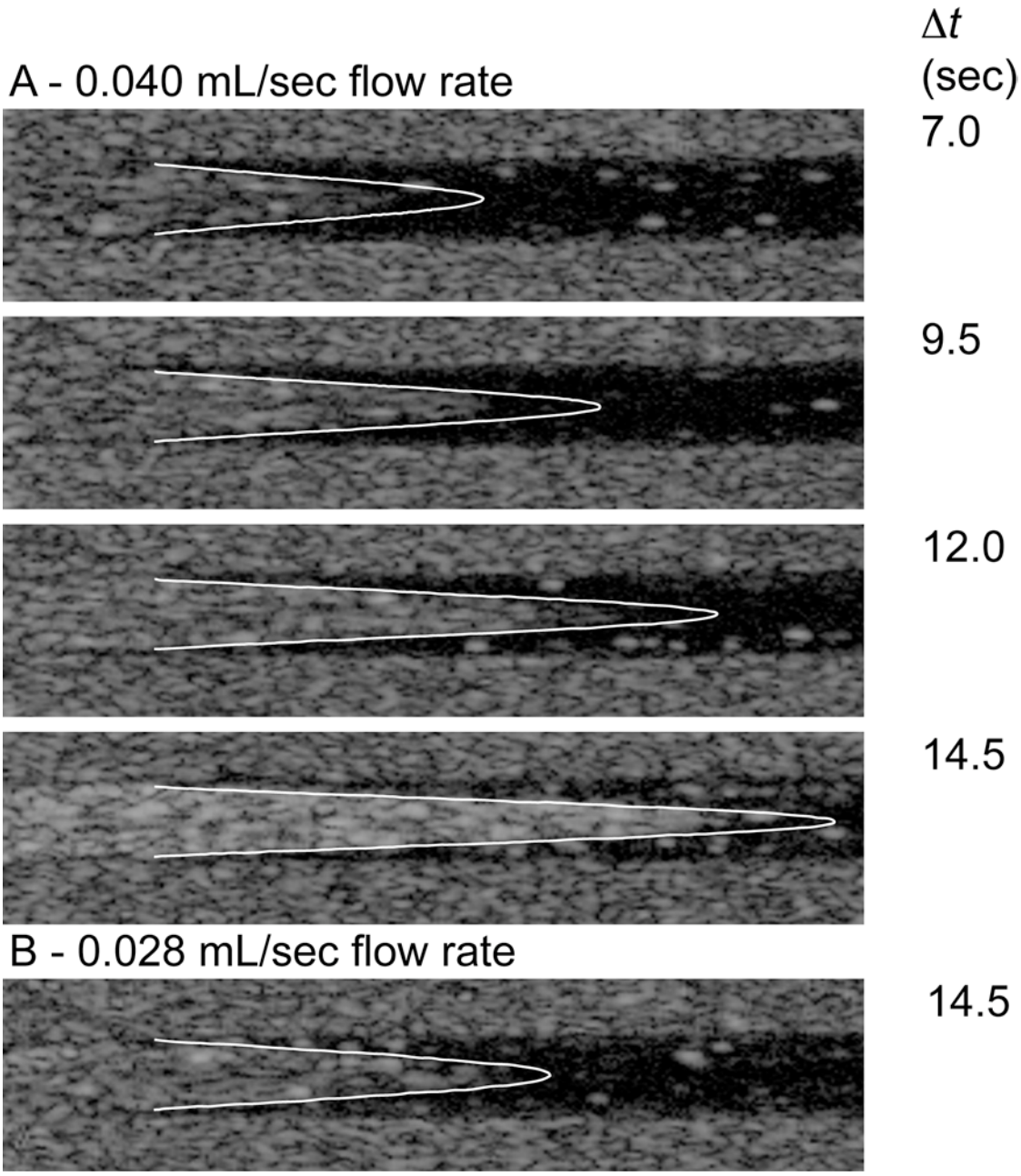
Δt
(sec)
A - 0.040 mL/sec flow rate
7.0
9.5
12.0
14.5
B - 0.028 mL/sec flow rate
14.5

Fig. 5.

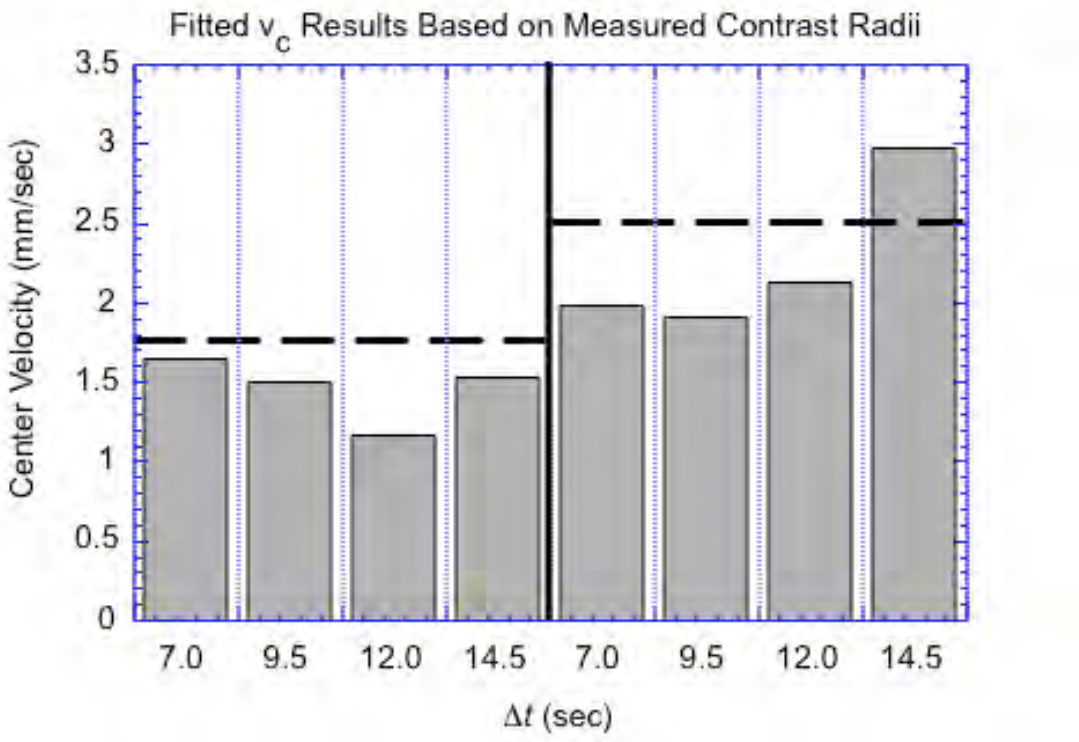
Fitted v_c Results Based on Measured Contrast Radii
Center Velocity (mm/sec)
3.5
3
2.5
2
1.5
1
0.5
0
7.0
9.5
12.0
14.5
7.0
9.5
12.0
14.5
Δt (sec)

Fig. 6.

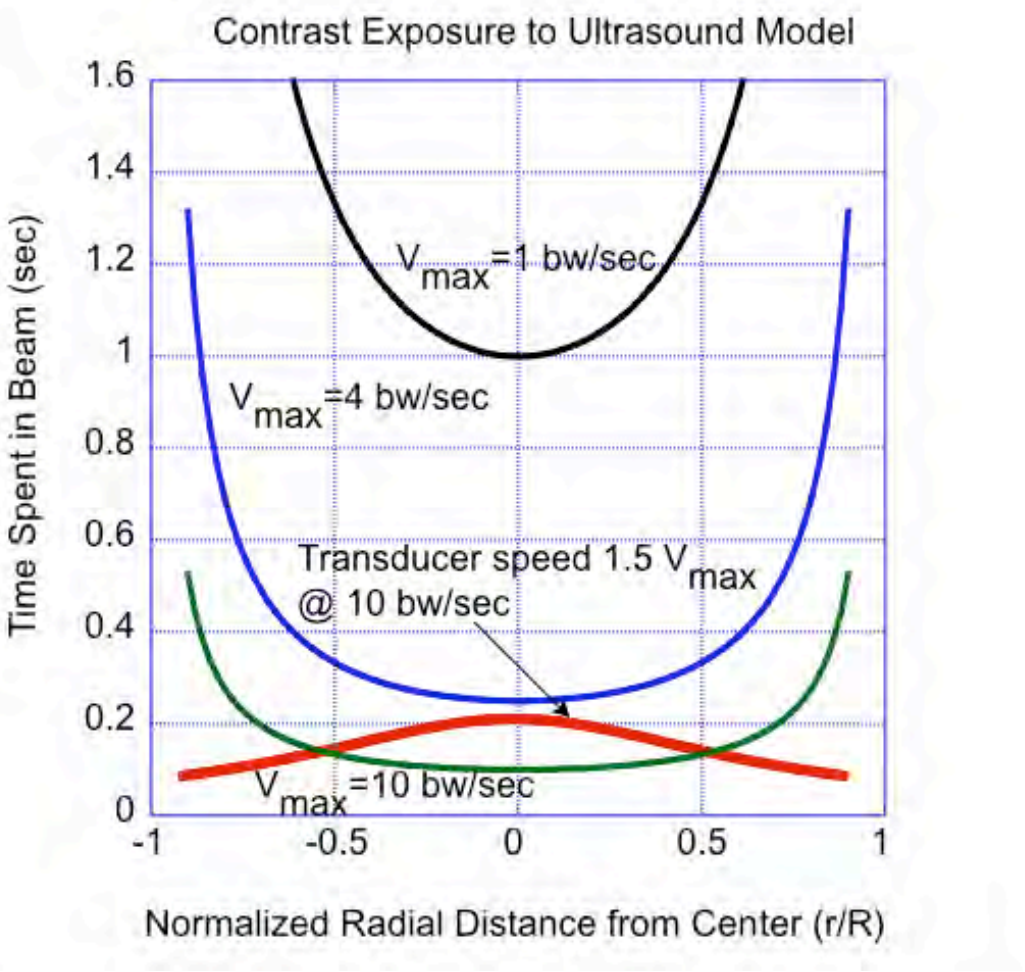
Contrast Exposure to Ultrasound Model
Time Spent in Beam (sec)
1.6
1.4
1.2
1
0.8
0.6
0.4
0.2
0
-1
-0.5
0
0.5
1
Normalized Radial Distance from Center (r/R)
Vmax=1 bw/sec
Vmax=4 bw/sec
Transducer speed 1.5 Vmax
@ 10 bw/sec
Vmax=10 bw/sec

Fig. 7.

Rapid 3D Imaging of Contrast Flow II: Application to Perfused Kidney Vasculature

Chen NG†, Fowlkes JB†‡, Carson PL†‡, LeCarpentier GL‡

Departments of Biomedical Engineering†/Radiology‡, University of Michigan, Ann Arbor, MI, USA

Please send all correspondence to:

Gerald L LeCarpentier, PhD

University of Michigan Dept of Radiology

Basic Radiological Sciences

200 Zina Pitcher Place Rm 3315

Ann Arbor, MI 48109-0553

(734) 647-9326 (Telephone)

(734) 764-8541 (FAX)

gllec@umich.edu

Rapid 3D Imaging of Contrast Flow II: Application to Perfused Kidney Vasculature

Abstract

As noted in Part I of this study, refill imaging of ultrasound contrast in a 3D volume is potentially superior to 2D imaging for vascular characterization. A dual plane, dynamic refill technique was used to image a preserved porcine kidney perfused with contrast. For a 4.7 x 5 x 9 cm^3 volume, high-speed 3D refill imaging for 7 time-point measurements up to 288 seconds was effective with an imaging time reduction of 96% over corresponding real-time imaging. Mean transit times (MTTs) were estimated for regions of interest (ROIs) within renal cortex in both cross-sectional and longitudinal planes extracted from reconstructed volumes. MTTs for these ROIs were also obtained using conventional means for comparison. After correcting for contrast degradation over time, dual beam measurements were statistically equivalent to those conventionally obtained. These experiments demonstrate that this dual beam technique effectively images 3D contrast refill in greatly reduced time.

Keywords: contrast refill, perfusion, blood flow, imaging, vasculature, angiogenesis, time-intensity curve

Introduction

Refill imaging of ultrasound contrast agent perfusion in a three-dimensional volume may allow superior vascular characterization of tissues when compared to two-dimensional imaging (Carson et al. 1999). Visualization and mapping of the blood flow within and surrounding tumors may provide a means for differentiating between benign and malignant masses (Bhatti et al. 2001; LeCarpentier et al.1999). After contrast is cleared from a volume, its refill can be monitored. For any given region of interest, signal intensities can be plotted as a function of refill time and fitted to a time-intensity curve from which the contrast mean transit time (MTT) can be estimated.

As previously described in part I (Chen et al. 2005), both traditional real-time refill imaging and interval imaging of contrast refill are impractical in three-dimensions since each slice plane has to be separately acquired for the duration of the refill. The number of slices needed to constitute a three-dimensional volume is significant, and the net acquisition time is the product of that number and the time needed to acquire a single slice. This dependence would lead to excessive scan time requirements, during which the volume would need to be perfused with contrast agent.

The dual-transducer technique illustrated in part I (Chen et al. 2005) is one dual-beam method for collection of three-dimensional data. Sweeping a transducer pair, composed of a clearance transducer and a low-power imaging transducer as a unit at velocity v over a contrast perfused tissue volume collects the refill images of the entire volume at a refill time. Slice separation is determined by both the trigger rate of the imaging transducer and the translation velocity v as described in the appendix of part I (Chen et al. 2005) and has a minimal effect on acquisition time.

In order to test the effectiveness of a dual-beam method in imaging a perfused vascular bed, a preserved porcine kidney is used as a three-dimensional phantom (Holmes et al. 1984). Such a phantom contains a vascular bed and provides an environment to test the dual transducer technique with a more realistic spatial distribution of flow than the cylindrical tube phantom previously reported (Chen et al. 2005). Comparison of MTTs obtained in dual transducer acquisitions with those using real-time (Porter et al. 1999; Simpson et al. 1998) and interval imaging (Kamiyama et al. 1996; Moriyasu et al. 1996; Ohmori et al. 1997; Wei et al. 1998) can be used to demonstrate the efficacy of a dual-beam method. Validation of the three-dimensional nature of the acquisition is performed by examining the images in the lateral-elevational plane of the dual transducer acquisitions and comparing those images to corresponding images directly acquired.

Theoretical Considerations

In a perfused vascular bed, contrast agent fills the blood vessels, and it is assumed that the agent follows the fluid flow perfusing the bed. Immediately after contrast clearance and the cessation of the high-powered insonation, contrast from outside the disruption zone begins to refill the cleared volume. The refill can be measured either continuously with low-power pulses (real-time refill imaging) or intermittently at only specified times. Alternatively, the refill can be imaged at high power at specified intervals, the contrast being cleared after each acquisition for the next time point to be measured (interval imaging). The contrast signal intensity (assumed proportional to the contrast concentration) at the measured time points can then be fitted to an exponential equation of the form $y(t) = A[1-\exp(-t/MTT)]$, where A is the

signal value at the asymptotic limit, *t* the time interval, and *MTT* the mean transit time (Wei et al. 1998). Differing flow dynamics would result in different MTT values, while the value of *A* depends on the contrast agent and its tissue concentration, and is assumed independent of the flow itself.

Experimental Methods

Ultrasound scans were conducted within a tank lined with sound absorbent rubber and filled with water that had been allowed to come to gas saturation. A schematic of the experimental setup is shown in Figure 1. The kidney (preserved as described below) was mounted beneath the water on a stand and secured with two rubber bands. As previously described in part I (Chen et al. 2005), a dual transducer assembly was used to demonstrate the dual beam technique by controlling both transducer separation and translation along the transducers' elevational direction. The transducer assembly was mounted upon a second stand that placed the transducers above the kidney being scanned.

A porcine kidney was obtained and preserved (Holmes et al. 1984) and subsequently rehydrated and degassed by perfusion through the renal artery with (> 5 L) degassed water. The kidney was subsequently perfused with a 1:5000 Definity/water suspension at 33 mL/min using a peristaltic pump (Cole-Parmer L/S pump and drive, Cole-Parmer Instrument Corporation, Barring, IL, USA). Dual transducer scans in the transverse orientation as shown in Figure 2 were made with the Toshiba Powervision (Toshiba Corporation, Otawara-shi, Tochigi-Ken, Japan) system using the PVN-375AT transducer for contrast clearance. In order to consistently adjust power output and firing

rate, the transducer was placed in harmonic mode (power setting of P8 at a frame rate of 10 Hz). The GE Logiq 9 (General Electric Corporation, Milwaukee, WI, USA) 7L transducer in phase inversion (PI) mode at low power (2% acoustic output-AO) was the imaging transducer. Images for a 90 mm thick volume of interest for refill times of 16, 32, 48, 96, 144, 288, and 432 sec with a 1 mm slice separation were acquired. The GE Logiq 9 was specifically adapted to store triggered images into the cine buffer through the opening and closing of its footswitch control. As the transducer was translated, slice separation was controlled by opening and closing the control with a solid-state relay (manufacturer and model) with a LabVIEW (National Instruments Corporation, Austin, TX, USA) script. For the translation speed of 6 mm/sec, a triggering rate of 6 Hz provided the 1 mm slice separation in the acquisitions. In addition, a set of sparsely acquired dual-transducer images were taken with a slice separation of 20 mm in order to demonstrate the independence of the refill behavior from the slice spacing.

Refill data using real-time and interval imaging methods were collected using the GE L9 at a single slice position in the transverse orientation for comparison with dual transducer results. Using the footswitch trigger, fifty clearance pulses at 5 Hz were fired at high power (100% AO), and images subsequently collected at 2% AO at a 1 Hz frame rate for real-time refill. Interval imaging was performed using the same clearance pulse sequence, and imaging of contrast signal for different intervals at both 2% and 100% AO. The measured signal intensities for the kidney perfused with water (no contrast) were then subtracted from those of the other images, and fitted to the exponential equation $f(t)=A[1-exp(-1/MTT)]$ for a region of interest in the kidney cortex and compared among the different methods.

A slice in the longitudinal direction was imaged using interval imaging and real-time refill for comparison with a longitudinal image plane extracted from the 3D volume acquired with the dual transducer technique to demonstrate its 3D capabilities. The extracted images in the longitudinal orientation corresponding to those directly acquired were selected using image registration with MIAMI Fuse software developed at the University of Michigan (Meyer et al. 1997; Meyer et al. 1999). Mean transit times for a region of interest were recorded for each technique and compared.

Results

Representative images indicated in Figure 3 show a selected transverse slice (i.e. with slice orientation as those acquired by the dual transducer (DT) method) imaged using both interval imaging (II) and real-time refill (RT) compared with corresponding DT images. Figure 4 shows some representative refill curves corresponding to the images. In Figure 5A, the estimated MTT values are compared for data acquired using each method, and the values follow a clear trend. Dual transducer measurements were shorter than those otherwise measured but were consistent with each other. The MTT for the DT sparse case is comparable to the other DT MTT measurements, indicating that slice spacing did not affect the DT measurement results. The MTT for the II sequence taken at 100% AO had a shorter MTT than that taken at 2% AO, and both were shorter than those acquired using RT.

The elevation in MTTs measured through real-time refill relative to data obtained otherwise was possibly due to a slight decrease in overall contrast signal level over the course of each experiment. Such a decay in contrast signal would cause a decrease in

MTT measured with II at 2% AO, which requires a relatively long time to acquire and would otherwise be expected to match the RT measured value. Contrast degradation is minimal for RT acquisitions since any time point being measured requires only the elapsed time from the end of the contrast clearance sequence. For example, the time point of 288 sec requires only 288 sec of elapsed time. On the other hand, for the II case where the time points were acquired sequentially, the same 288 sec (4.8 min) time point would be acquired 714 sec (11.9 min) after initial contrast clearance at the start of the experiment since there was acquisition time associated with all the other time points measured. The DT scans require similar times as II; however it should be noted that the refill imaging for the entire volume is performed during that time, as opposed to a single slice plane acquisition in the case of RT and II.

Contrast degradation over time can be modeled as a decaying exponential of the form $y(t)=Ae^{-\beta t}$, with a constant β, which corresponds to a fixed percentage of contrast signal per unit time. A slight decrease in contrast signal over time would skew the MTT curve fit by artificially depressing the latter data points as shown in Figure 6A. Further evidence for a slight decrease in signal level over time is found in the signal level ratios shown in Table 1. The ratios are approximately identical at short times, but they diverge at longer time points. Since the longer time points for II and DT are acquired at times significantly longer than those of RT post-infusion, slight contrast degradation with time would be consistent with this divergence in ratios.

One can compensate for the contrast decay by normalizing the measured signal intensities by $e^{-\beta t}$ for the times *t* at which the images were collected. Since the refill dynamics for the RT measurements and their corresponding II taken at an acoustic

output of 2% are identical, the measured MTTs should be statistically identical. The difference in their directly measured values can be ascribed to the contrast decay and used to estimate the contrast decay over time by determining the correction factor that would statistically equalize the MTTs. It was found that a correction factor of 4.1% per minute applied to both the RT and II measurements would cause the mean RT MTT to fall within the 95% confidence interval of the II measurement. Correction factors for the other acquisitions that would equalize the measured MTTs to statistical significance are indicated in Figure 5B.

Dual transducer images were assembled to form three-dimensional images of the kidney for each acquisition time point. Representative reconstructed slices corresponding to those directly acquired perpendicular to the dual-transducer images, as well as those directly acquired images, are shown in Figure 7. For the marked ROI, the measured MTTs for each technique follow the trend for the transverse case, and can likewise be corrected to approximately equal values as shown in Figure 8. The successful image reconstruction and MTT correspondence with directly acquired data demonstrate the ability of the DT technique to generate true 3D refill data.

Conclusions and Discussion

We have demonstrated the efficacy of a new technique in contrast refill imaging. The dual transducer technique allows the imaging of contrast destruction/refill data in a three-dimensional volume in a drastically reduced time frame, compared to traditional techniques (real-time refill and interval imaging). The ability of the dual transducer technique to obtain mean transit time (MTT) measurements similar to those of

conventional methods but in a fraction of the time, and to generate meaningful longitudinal images perpendicular to the scan direction suggests this technique is useful in imaging the vasculature of perfused tissue on a three-dimensional basis.

Due to the restrictions on contrast flow rate associated with the perfused kidney phantom used here, contrast decay unfortunately plays an important role in skewing measured MTTs. However in clinical practice contrast decay effects would be negligible *in vivo* where the MTTs measured are typically much shorter (such as those from Seidel et al. 1999) the effect of which is shown in Figure 6B. In addition, if necessary, any decay could be readily corrected by monitoring the decay via a major vessel. Nevertheless, the dual transducer measurements were consistent with each other without correction, and at the very least provided a measure of relative MTT.

Correction factors that would statistically equalize (as previously described) the RT measured MTTs with the DT scans and II at 100% AO scan were also computed and are indicated in Figures 5B and 8B. However, the DT and II MTTs may *indeed* differ from RT MTTs due to differing flow dynamics. The DT technique clears the entire volume of interest of contrast before imaging the refill as opposed to RT, where only a single slice plane is cleared prior to imaging. In II at 100% AO, there is the same contrast clearance pattern as RT; however, the slice thickness of the imaging plane may be broader due to the increased acoustic output used, causing contrast to refill the imaging plane sooner and reducing MTT. These differences, which are not accounted for here, could affect measured MTTs in addition to contrast degradation.

Image quality of the longitudinal images obtained using the dual transducer technique is limited only by the acquisition frame rate and the transducer elevational

point-spread function. Our previous work with this transducer (unpublished observations) suggests that longitudinal image quality is not appreciably improved at a slice separation below ~500 μm, which can be readily achieved with the dual transducer technique with no increase in scan time requirements.

We have shown previously that the technique gives expected results in a laminar tube flow (Chen et al. 2005) and now in a preserved kidney phantom. The DT technique is only one of several possible dual beam methods that could be used to image a three-dimensional volume. With a two-dimensional array, mechanical translation can become unnecessary and acquisition times reduced from those needed by the DT technique demonstrated here. The dual-beam techniques can readily be applied toward living tissues with their higher flow rates and hence shorter MTTs, thereby avoiding all contrast degradation issues, to produce a practical means of obtaining three-dimensional contrast perfusion images.

Acknowledgement

This project was sponsored by the US Army under grant DAMD17-01-1-0327 and R01-DK56658 from the US National Institutes of Health (NIH). Kimberly Ives, DVM kindly assisted in the acquisition and preparation of the porcine kidney. Dr. Huzefa Neemuchwala kindly assisted in providing scripts used in preserving proper image aspect ratios, and Sakina Zabuawala assisted in the use of MIAMI Fuse.

References

Bhatti PT, LeCarpentier GL, Roubidoux MA, et al. Discrimination of Sonographic Breast Lesions Using Frequency Shift Color Doppler Imaging, Age and Gray Scale Criteria. J Ultrasound Med 2001; 20:343-350.

Carson PL, Moskalik AP, Govil A, et al. The 3D and 2D Color Flow Display of Breast Masses, Ultrasound Med Biol 1997; 23(6) 837-849.

Chen NG, Fowlkes JB, Carson PL, LeCarpentier GL. High Speed 3D Imaging of Ultrasound Contrast Flow Dynamics Part I: Demonstration of a dual Beam Technique. Ultrasound Med Biol 2005 (submitted).

Holmes KR, Ryan W, Weinstein P, Chen MM. A fixation technique for organs to be used as perfused tissue phantoms in bioheat transfer studies. ASME ADV BIOENG, 1984; 9-10.

Kamiyama N, Moriyasu F, Kono Y, et al. Investigation of the “flash echo” signal associated with a US contrast agent. Radiology 1996; 201(165).

LeCarpentier GL, Bhatti PT, Fowlkes JB, et al. Utility of 3D Ultrasound in the discrimination and detection of breast cancer. RSNA EJ, 1999; http://ej.rsna.org/ej3/0103-99.fin/titlepage.html.

Meyer CR, Boes JL, Kim B, et al. Demonstration of accuracy and clinical versatility of mutual information for automatic multimodality image fusion using affine and thin plate spline warped geometric deformations. Med Image Anal 1997; 1(3) 195-206.

Meyer CR, Boes JL, Kim B, et al. Semiautomatic Registration of Volumetric Ultrasound Scans. Ultrasound Med Biol 1999; 25(3): 339-347.

Moriyasu F, Kono Y, Nada T, et al. Flash echo (passive cavitation) imaging of the liver by using US contrast agents and intermittent scanning sequence. Radiology 1996; 201(374).

Ohmori K, Cotter B, Kwan OL, Mizushige K, DeMaria A. Relation of contrast echo intensity and flow velocity to the amplification of contrast opacification produced by intermittent ultrasound transmission. Am Heart J 1997; 134: 1066-1074.

Porter TR, Li S, Jiang L, Grayburn P, Deligonul U. Real time visualization of myocardial perfusion and wall thickening in humans with intravenous ultrasound contrast and accelerated intermittent harmonic imaging. J Am Soc Echocardiogr 1999; 12: 266-71.

Seidel G, Greis C, Sonne J, Kaps M. Harmonic grey scale imaging of the human brain. J Neuroimaging 1999; 9(3): 171-174.

Simpson DH, Burns PN. Perfusion imaging with pulse inversion Doppler and microbubble contrast agents: in vivo studies of the myocardium. IEEE Ultrason Symposium 1998; 2: 1783-1786.

Wei K, Jayaweera AR, Firoozan S, et al. Quantification of Myocardial Blood Flow With Ultrasound-Induced Destruction of Microbubbles Administered as a Constant Venous Infusion. Circulation 1998; 97(5): 473-483.

Time (sec)	Real-time		Interval Imaging (2% AO)		Dual-Transducer	
	R_{sig}	t_{acq} (sec)	R_{sig}	t_{acq} (sec)	R_{sig}	t_{acq} (sec)
16 (ref)	1	16	1	31	1	60
32	2.00	32	2.06	78	2.13	180
48	3.47	48	3.33	141	2.80	300
96	6.59	96	5.20	252	4.49	480
144	8.60	144	6.64	411	4.56	720
288	12.97	288	7.90	714	4.42	1140

Table 1 - Ratio of measured signal intensity relative to reference time point at 16 sec. The ratios are approximately equal for all methods for short intervals, yet diverge with longer time intervals. This divergence is most pronounced for dual transducer data since the DT technique requires the most time, although it is also significant for the interval imaging case. The signal reduction only at longer time points is consistent with a gradual loss of contrast signal strength that would explain the systematic reduction in measured MTT using the II and DT techniques. For actual studies *in vivo*, time-dependent contrast degradation would not be significant because the necessary measurement times would be much shorter (see discussion).

Figure 1 - Schematic of dual-transducer apparatus and experimental setup. The dual-transducer apparatus (modified from the apparatus previously reported) consists of a dual-transducer positioning stage, which consists of translation (M_T) and separation (M_S) motors. Each motor turns a threaded rod, which translates a platform that contains a transducer holder. The platforms translate within the tracked slide. Motors are connected to a powered control module, which contain the electronics driving the motors. The control module is linked to a laptop computer through the DAQCard-700. The control module also contains circuitry needed to operate the footswitch trigger and is linked to the GE (General Electric Corporation, Milwaukee, WI, USA) Logiq 9 footswitch control in order to trigger image acquisition. Using LabVIEW scripts, the imaging transducer (T_i) is triggered and transducers translated as required. The transducers are positioned above the phantom being scanned, with the clearance transducer (T_c) positioned at the edge of the volume of interest. The phantom is continuously perfused with dilute (1:5000 concentration) contrast pumped from a stirred flask.

Figure 2 - Kidney phantom with transducer orientations. The kidney phantom is perfused through the renal artery that is connected to a pump. All dual transducer scans are acquired by translating the transducers as indicated by the arrows, with the transducers oriented in the transverse orientation. For comparison with reconstructed images acquired with the dual transducer technique, the imaging transducer was oriented in the longitudinal orientation perpendicular to the transverse orientation as shown.

Figure 3 - Representative transverse images obtained for a representative slice from preserved porcine kidney with interval imaging, real-time refill, and the dual transducer technique for refill times of 0, 16, and 288 sec. Images from real-time refill and dual transducer are obtained with the same acoustic settings as the 2% acoustic output interval imaging data. Interval imaging images obtained at 100% acoustic output are brighter because of the high transducer output used to obtain the images. Contrast clearance was obtained for both interval imaging cases and real-time refill using 50 pulses at 5 Hz at an acoustic output of 100%. The separate clearance transducer provided contrast clearance for the dual-transducer measurements. A rectangular window marks the region of interest in subsequent mean transit time comparisons.

Figure 4 - Example of measured refill curves. Abbreviations used are as follows: II - Interval Imaging, RT - Real-Time refill, DT - Dual Transducer technique, MTT - Mean Transit Time. Real-time refill imaging provides nearly continuous data for the ROI. Interval imaging and the dual transducer technique provide measurements at specific time points only; however, with a judicious selection of measured points, the MTT can be estimated. The II acquisition was obtained at an acoustic output of 2%. An image was obtained for the II case at 432 sec; however, its corresponding point (255) was excluded because including it would dramatically increase the sum of the squares of the errors (480 vs. 15054). Therefore, the data point was considered an outlier. Fitted MTT results (in sec) for these curves are RT - 182.23, II - 101.44, and DT - 44.55. The earlier

saturation and subsequent signal drop of the II and DT cases are probably due to contrast degradation over time.

Figure 5 - (A) Comparison of data obtained for a given transverse slice, with the ROI (regions of interest) indicated in Figure 8. Numerals refer to repeated acquisitions using the stated method (e.g. DT 3 - third acquired dual transducer data set). Error bars indicate the 95% confidence interval of the mean transit time value, as fitted to the expression *A[1-exp(-1/MTT)]* for measured data points. Percentages (for II) refer to the acoustic output (AO) used for readout after set of clearance pulses. Sparse refers to the acquisition where images were obtained at a large (20 mm) slice separation. DT measurements, although differing in absolute terms from corresponding measurements otherwise made, provide a consistent metric of MTT. (B) Factoring in the degradation of contrast agent signal with time, the MTTs can be corrected to values within statistical significance. Because the imaging and flow dynamics are identical for the RT measurements and the II measurement at 2% AO, the MTT should be identical for the measurements. Correcting the RT and II measurements with a contrast degradation factor of 4.1 percent per minute would make the II MTT value statistically equal to the mean of the RT measurements. Applying correction factors (in percent per minute) for the other measurements as indicated would cause the RT MTT mean to be within their 95% confidence interval.

Figure 6 - Effect of contrast decay. If contrast has a rate of decay proportional to the amount present, then its signal intensity would decrease exponentially with time. The

effect on measured MTTs however would only become apparent for experiments requiring relatively long acquisition times. The contrast signal reductions caused by this decay results in the apparent decrease in MTT. (A) Shown are the expected curves for refill dynamics that, with no decay, would result in a 150 sec MTT. Due to the time required to acquire the data set through interval imaging (the time points 16, 32, 48, 96, 144, 288, and 432 sec being acquired at 31, 78, 141, 252, 411, 714, and 1161 sec respectively after beginning acquisition), the observed results are significantly skewed, and without correction would produce a 75 sec MTT. DT acquisitions would also be affected due to their relatively long duration. (B) Contrast decay for short durations. For shorter experimental times, signal decay effects are barely noticeable, as signal level changes are primarily due to contrast fill. Shown here are an ideal refill curve with a 10 sec MTT, measured out to 30 sec and the corresponding II data for a 3%/min decay rate measured at 10, 20, and 30 sec time points for a total acquisition time of 60 sec. In contrast to the previous dramatic skewing of measured MTT, the measured MTT for the II measurement is 9.4 sec. Contrast decay is only significant in longer experimental acquisitions, and would likely be negligible *in vivo*, where experimental duration is significantly shorter.

Figure 7 - Representative longitudinal kidney images analogous to those in Figure 3. The kidney was rotated 90° and had interval refill data (at 100% and 2% acoustic output) and real-time refill measurements taken for the slice plane shown. Refill images for 0, 16, and 288 sec are displayed, with the ROI marked by a rectangular window. Contrast clearance was achieved with 50 100% AO pulses at 5 Hz. The dual transducer

images were obtained by stacking the transverse images from the dual-transducer scans in the elevational direction, and selecting the plane closest to that seen with the perpendicular scans through image registration with the MIAMI Fuse software. The images obtained are of a lower quality because of both the slice separation of 1 mm, and the transducer point-spread function in the elevational direction. However, one still observes contrast filling with time. The marked ROI is that which corresponds closest to the ROI marked in the directly acquired perpendicular images.

Figure 8 - (A) Comparison of mean transit time (MTT) data for perpendicular kidney images with the ROI as indicated in Figure 7. Recon refers to the images formed from the transverse dual transducer scans. MTT trends are identical to those in Figure 5 for analogous reasons. Dual transducer data was consistent among the three acquisitions. Error bars refer to the 95% confidence interval of the curve fit MTT. (B) Results obtained after applying a correction factor analogous to that in Figure 10B. Applying a correction for degradation of 5.3%/min makes the II curve acquired at 2% AO statistically equal to the mean of the corresponding RT measurements. The other measurements require correction factors as indicated to yield MTTs equal to the mean of the RT measurements.

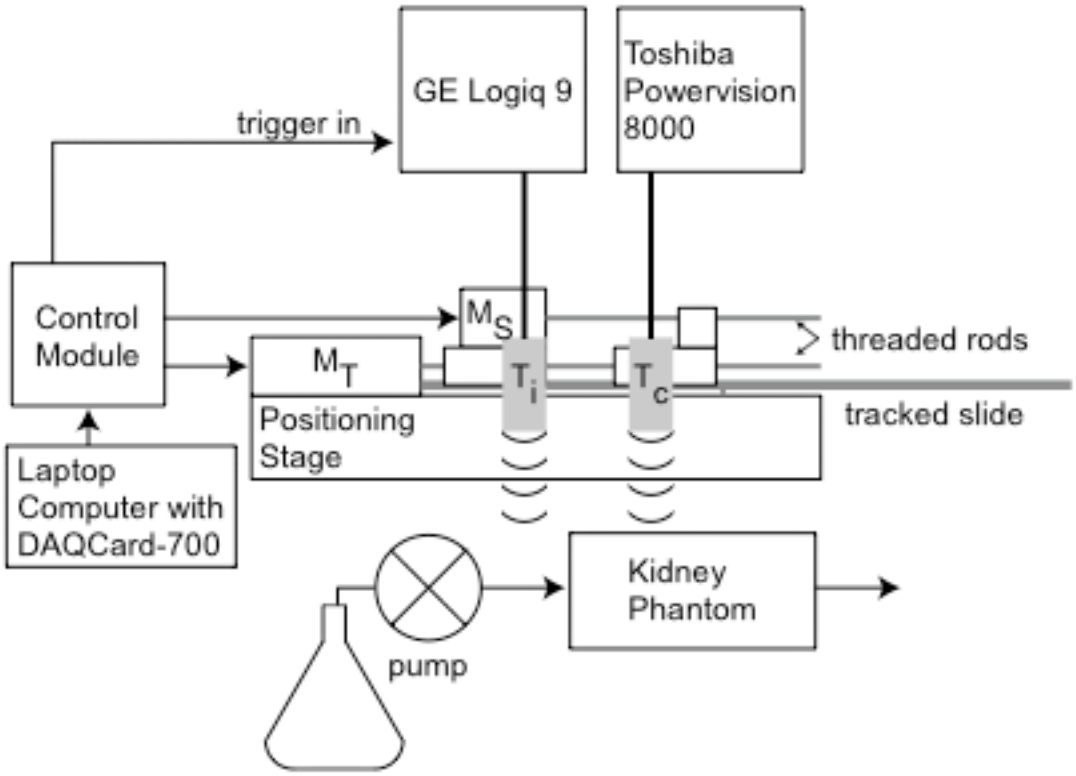
GE Logiq 9
Toshiba
Powervision
8000
trigger in
Control
Module
M_S
M_T
T_i
T_c
threaded rods
tracked slide
Positioning
Stage
Laptop
Computer with
DAQCard-700
Kidney
Phantom
pump

Fig. 1.

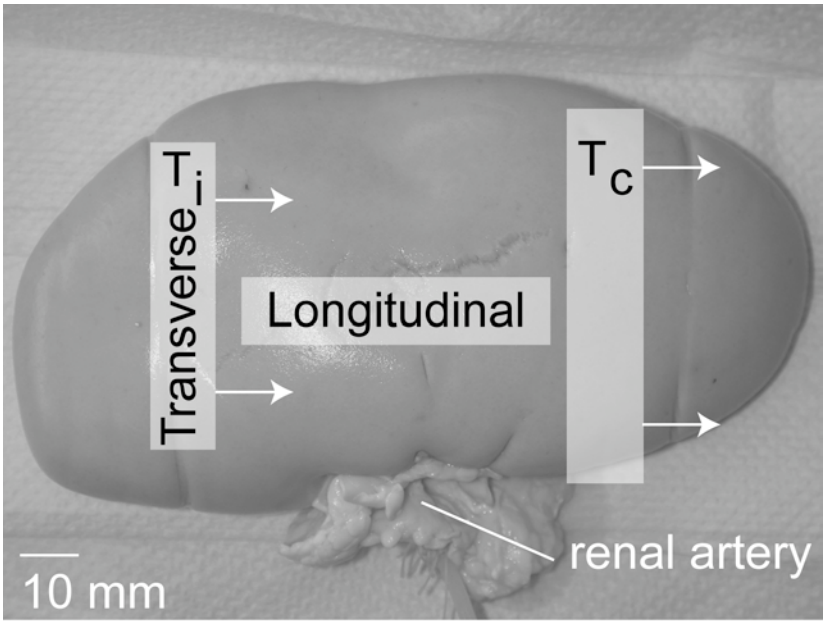

Fig. 2.

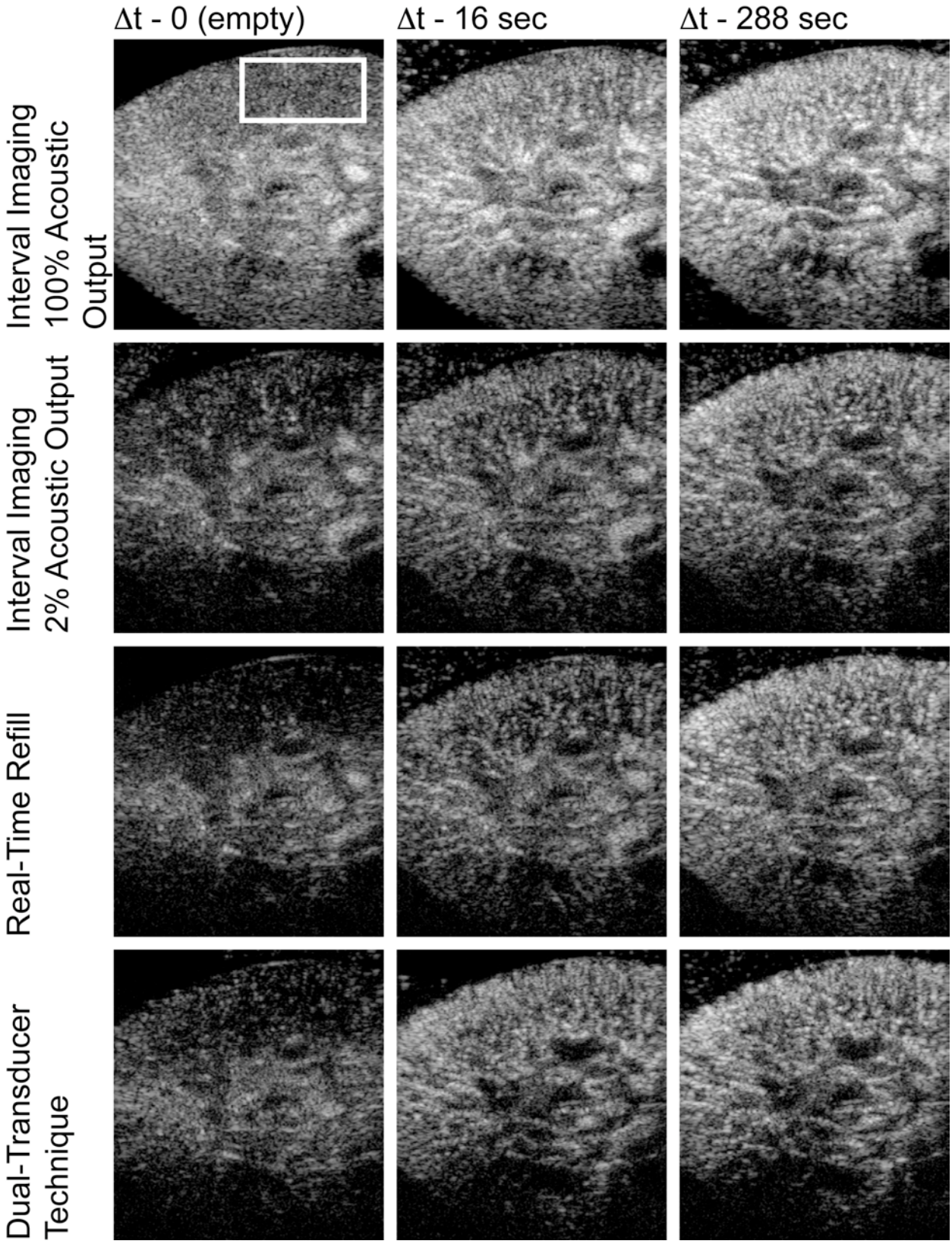
Δt - 0 (empty)
Δt - 16 sec
Δt - 288 sec
Interval Imaging 100% Acoustic Output
Interval Imaging 2% Acoustic Output
Real-Time Refill
Dual-Transducer Technique

Fig. 3.

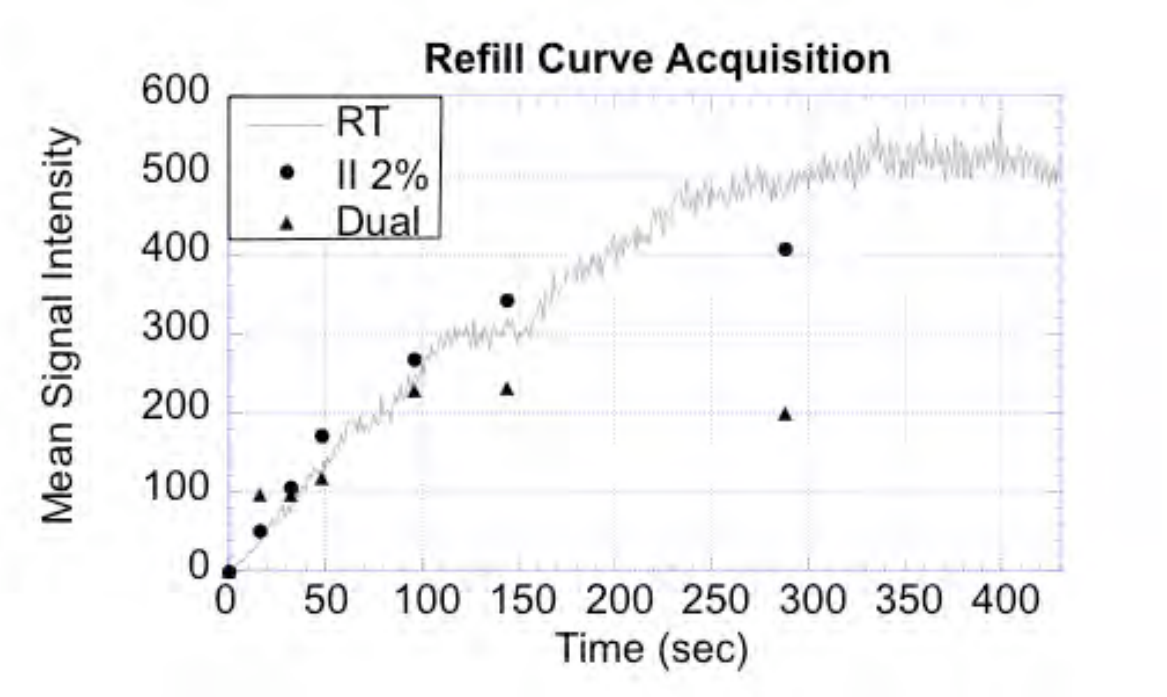
Refill Curve Acquisition
Mean Signal Intensity
600
500
400
300
200
100
0
RT
II 2%
Dual
0
50
100
150
200
250
300
350
400
Time (sec)

Fig. 4.

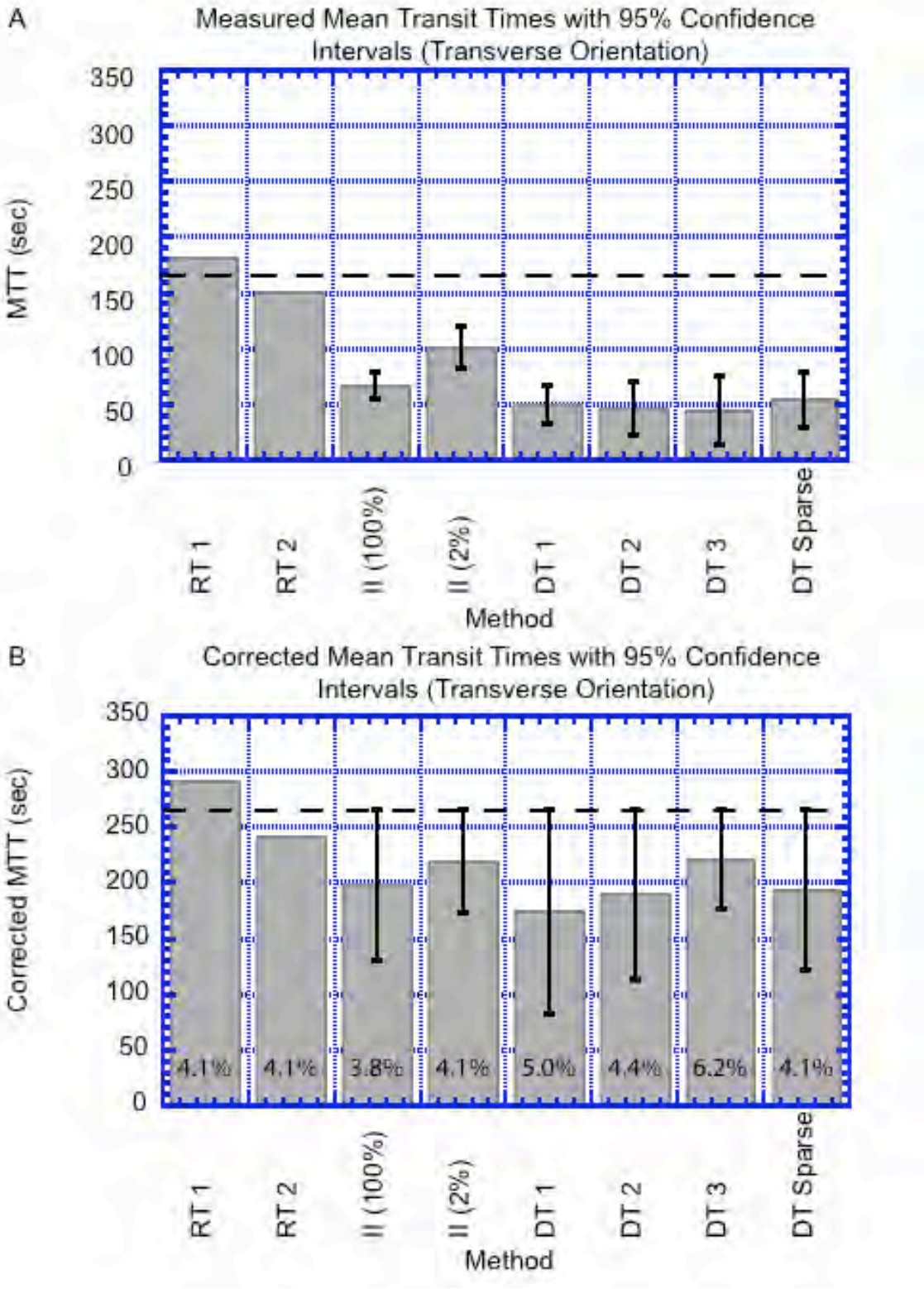
A
Measured Mean Transit Times with 95% Confidence Intervals (Transverse Orientation)
MTT (sec)
350
300
250
200
150
100
50
0
RT 1
RT 2
II (100%)
II (2%)
DT 1
DT 2
DT 3
DT Sparse
Method
B
Corrected Mean Transit Times with 95% Confidence Intervals (Transverse Orientation)
Corrected MTT (sec)
350
300
250
200
150
100
50
0
4.1%
4.1%
3.8%
4.1%
5.0%
4.4%
6.2%
4.1%
RT 1
RT 2
II (100%)
II (2%)
DT 1
DT 2
DT 3
DT Sparse
Method

Fig. 5.

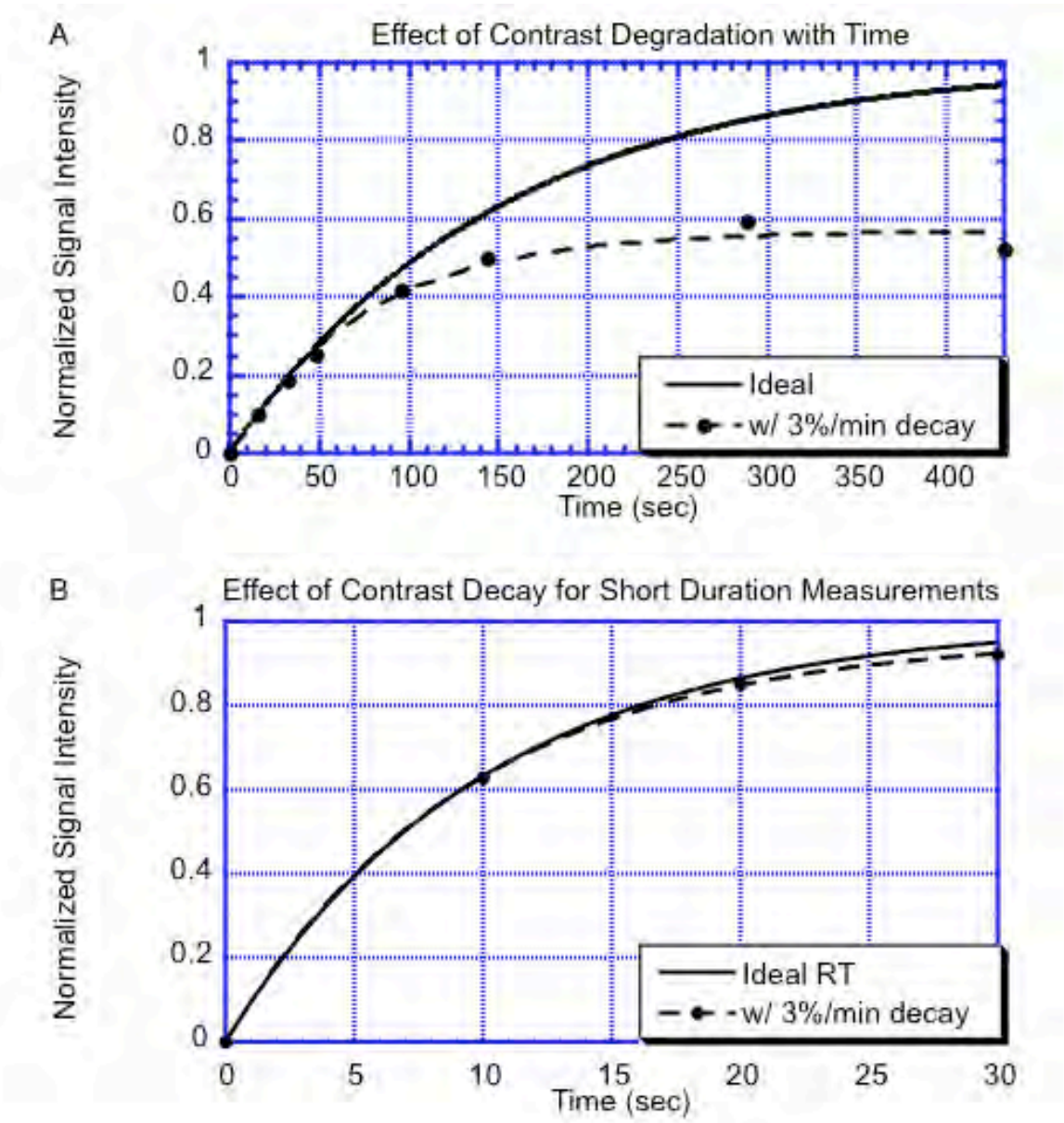
A
Effect of Contrast Degradation with Time
Normalized Signal Intensity
1
0.8
0.6
0.4
0.2
0
0
50
100
150
200
250
300
350
400
Time (sec)
Ideal
w/ 3%/min decay
B
Effect of Contrast Decay for Short Duration Measurements
Normalized Signal Intensity
1
0.8
0.6
0.4
0.2
0
0
5
10
15
20
25
30
Time (sec)
Ideal RT
w/ 3%/min decay

Fig. 6.

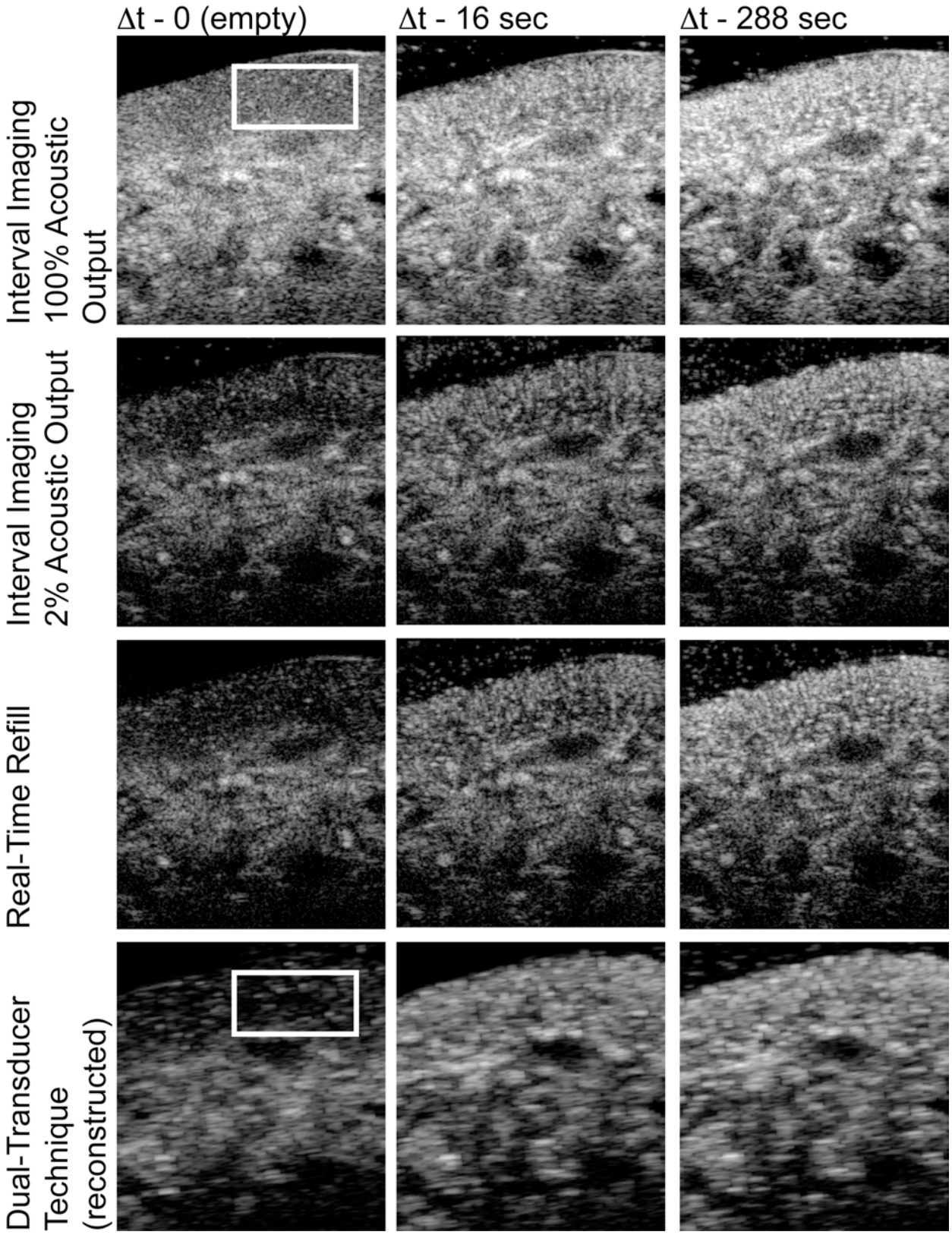
Δt - 0 (empty)
Δt - 16 sec
Δt - 288 sec
Interval Imaging 100% Acoustic Output
Interval Imaging 2% Acoustic Output
Real-Time Refill
Dual-Transducer Technique (reconstructed)

Fig. 7.

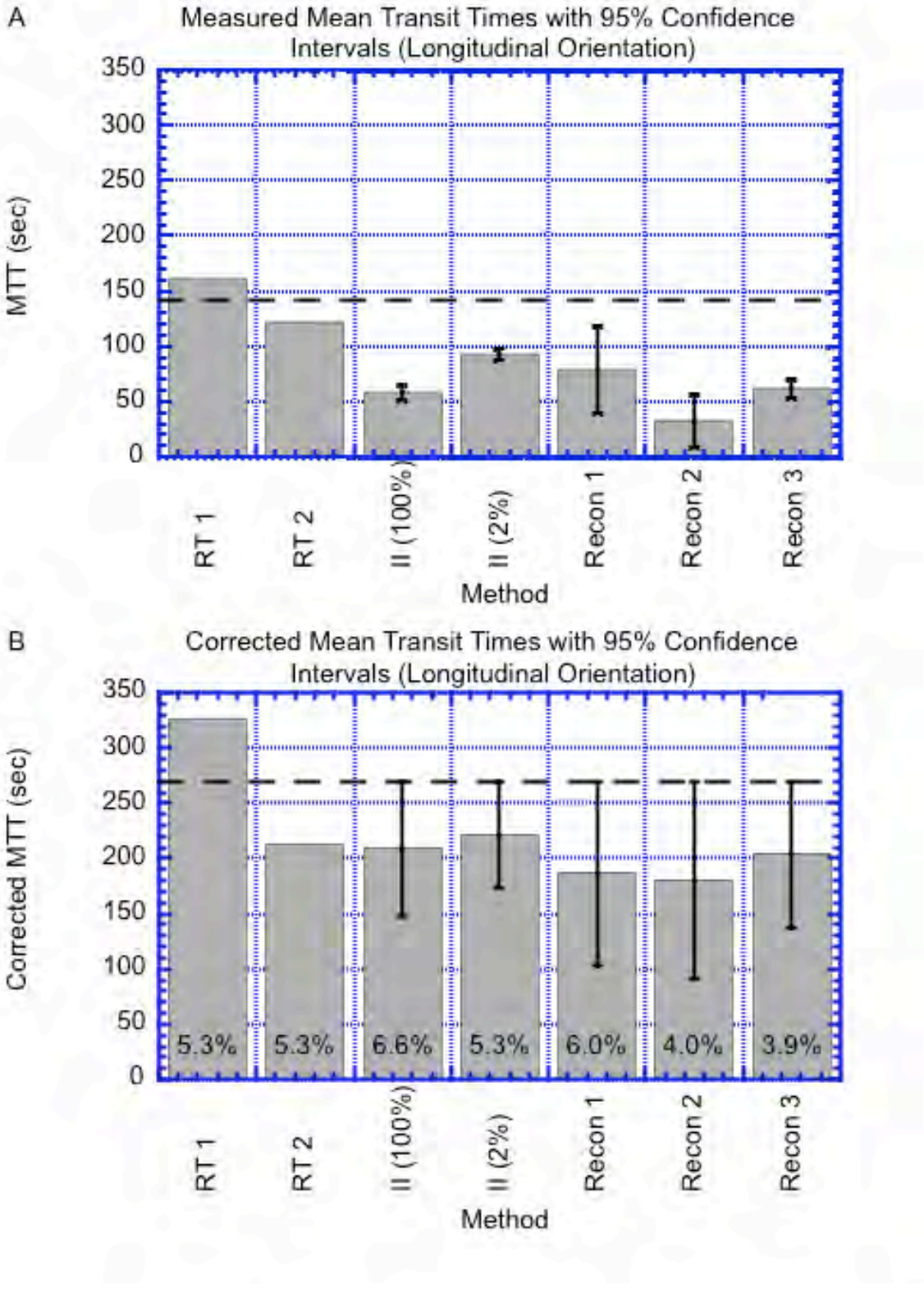
A
Measured Mean Transit Times with 95% Confidence Intervals (Longitudinal Orientation)
MTT (sec)
350
300
250
200
150
100
50
0
RT 1
RT 2
II (100%)
II (2%)
Recon 1
Recon 2
Recon 3
Method
B
Corrected Mean Transit Times with 95% Confidence Intervals (Longitudinal Orientation)
Corrected MTT (sec)
350
300
250
200
150
100
50
0
5.3%
5.3%
6.6%
5.3%
6.0%
4.0%
3.9%
RT 1
RT 2
II (100%)
II (2%)
Recon 1
Recon 2
Recon 3
Method

Fig. 8.